



Université du Québec
à Rimouski

Stratigraphie et processus sédimentaires dans le chenal de navigation du Port de Montréal

Mémoire présenté

dans le cadre du programme de maîtrise en océanographie

en vue de l'obtention du grade de maître ès sciences

PAR

© Simon Nadeau

Octobre 2019

Composition du jury :

Pascal Bernatchez, président du jury, UQAR

Guillaume St-Onge, directeur de recherche, UQAR-ISMER

Pierre Francus, examinateur externe, INRS-ETE

Dépôt initial le 12 juin 2019

Dépôt final le 23 octobre 2019

UNIVERSITÉ DU QUÉBEC À RIMOUSKI
Service de la bibliothèque

Avertissement

La diffusion de ce mémoire ou de cette thèse se fait dans le respect des droits de son auteur, qui a signé le formulaire « *Autorisation de reproduire et de diffuser un rapport, un mémoire ou une thèse* ». En signant ce formulaire, l'auteur concède à l'Université du Québec à Rimouski une licence non exclusive d'utilisation et de publication de la totalité ou d'une partie importante de son travail de recherche pour des fins pédagogiques et non commerciales. Plus précisément, l'auteur autorise l'Université du Québec à Rimouski à reproduire, diffuser, prêter, distribuer ou vendre des copies de son travail de recherche à des fins non commerciales sur quelque support que ce soit, y compris l'Internet. Cette licence et cette autorisation n'entraînent pas une renonciation de la part de l'auteur à ses droits moraux ni à ses droits de propriété intellectuelle. Sauf entente contraire, l'auteur conserve la liberté de diffuser et de commercialiser ou non ce travail dont il possède un exemplaire.

À tous ceux qui font le peu,
même le très peu, dont ils sont capables
pour préserver l'environnement, ceux
qui ont compris que l'idée d'une
croissance infinie sur une Terre finie est
une illusion sociale qui disparaîtra avec
ou sans nous...

REMERCIEMENTS

Je désire tout d'abord remercier mon directeur de recherche Guillaume St-Onge. Guillaume a accepté de me confier ce projet qu'il avait organisé avec le Port de Montréal alors qu'on ne s'était rencontré que par vidéo en direct sur Internet. Il m'a conseillé durant les trois années qu'a duré ma maîtrise. Son aide a été particulièrement importante, concernant le financement et la mise en œuvre du projet, faire le contact avec des personnes ressources et sa rigueur scientifique pour les corrections ou améliorations de mes différents travaux. Je veux aussi le remercier pour la latitude qu'il m'a laissée quant aux décisions entourant plusieurs aspects de ma recherche et la gestion de mon temps. Il a été à l'écoute des problèmes rencontrés et de leurs conséquences sur le déroulement du projet (santé, vacances, problèmes informatiques, salaire, bris de matériel, couts des travaux, etc.). Je tiens aussi à mentionner que ce projet n'aurait pas été réalisable sans la participation de toute l'équipe de la Chaire de recherche en géologie marine de l'UQAR-ISMER, ainsi que de plusieurs étudiants. Merci à : Claude Rouleau et Pascal Rioux pour les mesures des isotopes du ^{210}Pb , Marie-Pier St-Onge pour les analyses de granulométrie laser et pour plusieurs conseils techniques en laboratoire, Quentin Beauvais pour l'analyse des carottes au MSCL, son aide durant la mission et la correction des coordonnées de sismiques, Pierre-Arnaud Desiage pour les conseils techniques concernant la sismique et son aide durant la mission FJS2017, Édouard Philippe pour ses conseils techniques sur le traitement de données informatiques lourdes.

Je tiens ensuite à dire un merci tout particulier à Luc Dumontier, mon superviseur du stage au Port de Montréal. Luc a été comme un livre ouvert et a mis en œuvre toutes les ressources dont il disposait pour m'aider à avancer ce stage pré-maîtrise. Plusieurs autres employés du Port de Montréal ont également fait de ce stage une belle expérience. Je remercie particulièrement : François Valiquette, Christian Caron, Claude Deschambault, Alain Létourneau, Abdelhamid Riahi, Safa Boujida et Daniel Dagenais.

Je veux ensuite mentionner l'importance de certaines personnes m'ayant entouré lors de ces années d'étude, ainsi qu'au quotidien. Merci à Yan Lévesque de m'avoir parlé de cet institut de recherche, pour avoir été un compagnon d'études et un ami du baccalauréat jusqu'à maintenant. Merci à François Genin d'avoir aussi été un compagnon d'études à la maîtrise et un ami qui partage plusieurs de mes passions. Un très gros merci à Marie-Ève Lamarre pour avoir corrigé mon anglais très imparfait et pour être une compagne qui enjolive bien d'autres aspects de ma vie. J'éprouve une gratitude infinie envers ma famille qui m'a aidé de multiples façons et qui est en partie la cause de mes réussites... Merci à Andrée Miron et Laurice Nadeau, mes parents.

De nombreuses personnes ressources m'ont apporté une aide généreuse et le partage de leur expertise à différents moments lors de ce projet. Merci à : Antoine Morissette pour les conseils sur l'utilisation de jeux de données sur *ArcGIS*, le Service Hydrographique du Canada, et particulièrement à Jonathan Morin, pour leur professionnalisme, Mathieu Rondeau pour son aide avec le logiciel *Caris Hips & Sips*, Patrick Lajeunesse ainsi que son étudiante Annie-Pier Trottier pour leur soutien matériel essentiel à la mission FJS2017 et pour leurs conseils concernant la sismique, Alexandre Normandeau pour son expertise sur l'interprétation de la bathymétrie et de la sismique.

Finalement, je remercie la Ville de Verchères et sa marina pour leur collaboration à la mission FJS2017, le Ministère de l'Énergie et des Ressources Naturelles du Québec pour l'entente d'utilisation et de modification de la structure *ArcGIS* du SIGÉOM, le Centre Interdisciplinaire de Développement en Cartographie des Océans pour la location de leur bateau et le soutien technique de Sylvain Gauthier concernant l'organisation de la mission ainsi que les indications sur les instruments de levés scientifiques.

RÉSUMÉ

Une connaissance appropriée de la géologie entourant un port maritime international est requise pour assurer la sécurité du transport et des opérations de dragage. Un projet a été mis en place pour caractériser les sédiments, leur composition, les processus sédimentaires et la stratigraphie le long de la voie navigable du Port de Montréal. Une base de données géoréférencée a tout d'abord été développée à partir d'archives géotechniques. Elle intègre des milliers de descriptions de forages enregistrées depuis 1830. Une expédition a ensuite été réalisée à bord du navire scientifique F.J. Saucier. 148 km de profils acoustiques de sous-surface (3,5 kHz) et 27 carottes courtes de sédiments ont été acquis. L'analyse des données plurianuelles de la bathymétrie multifaisceaux fournis par le Service hydrographique du Canada révèle une érosion moyenne de 2,7 cm/an dans la voie navigable depuis les 12 dernières années. L'étude des dunes subaquatiques et des autres formes dénote un apport limité en sédiments. Cependant, la zone située entre le quai Jacques-Cartier et la fin des Îles de Boucherville est sujette à l'accumulation (jusqu'à 14 cm/an) et doit donc être surveillée. Les données sismiques combinées aux descriptions de forages et aux carottes sédimentaires indiquent l'affleurement du roc (Shale d'Utica) dans cette zone sensible. Le roc plonge ensuite devant l'Île Ste-Thérèse et les sédiments sus-jacents quaternaires apparaissent. Une sous-unité non laminée des argiles de la mer de Champlain affleure jusqu'au seuil de l'Île-aux-Prunes. Les carottes sédimentaires en aval de ce point sont clairement laminées et constituent une seconde sous-unité des argiles de la mer de Champlain. Tous les échantillons analysés en laboratoire présentent des caractéristiques similaires et typiques des argiles de la mer de Champlain. La distribution granulométrique est dominée par l'argile et le silt, avec des proportions variables de sable, de gravier et de cailloux. Les carottes dominées par des sédiments grossiers proviennent de champs de dunes et de zones d'érosion où les forts courants (~ 1 m/s) ont récemment transporté ces sédiments. Les teneurs en carbone total (0,5% à 2,3%) et en eau (36,0 ± 5,9%) des argiles sont normales pour un environnement marin. De plus, la datation au ^{14}C d'une coquille de pélécypode indique un âge de 11 640 cal BP et l'absence de ^{210}Pb en excès corrobore la tendance à l'érosion de la voie navigable.

Mots clés : Forage, stratigraphie, sismique, sédiments, port, Montréal, bathymétrie multifaisceaux, chenal de navigation, mer de Champlain.

ABSTRACT

A good understanding of the stratigraphy and the sedimentary processes are required to ensure the security of maritime transport and dredging operations around an international port. A research project was thus established to characterize the sediments, their composition and stratigraphy, and the sedimentary processes acting in the Port of Montreal and its waterway. A geodatabase was firstly developed from the geotechnical archives of the Port of Montreal and its partners. It integrates thousands of borehole descriptions recorded since 1830 AD. A sampling mission was then realised on board the scientific vessel F.J. Saucier. It resulted in the acquisition of 148 km of acoustic subbottom profiles (3.5 kHz) and 27 short sediment cores. The analysis of multiannual bathymetric multibeam echosounding data provided by the Canadian Hydrographic Service shows that a mean erosion trend of 2.7 cm/yr is occurring in the waterway since the last 12 years. The shapes and migration rates of subaqueous dunes and other submarine features also denote a low-supply sediment model. However, the area between the Jacques-Cartier wharf and the end of the Boucherville's Island is subject to accumulation (up to 14 cm/yr) and needs to be closely monitored. The seismic data combined to the ArcGIS borehole descriptions and the short sedimentary cores indicate outcropping of the bedrock (Shale of Utica) in this sensible area. The bedrock then plunges in front of the Ste-Thérèse Island and the Quaternary overlying sediments outcrop with an unlaminated subunit of the Champlain Sea Clays until a threshold in front of the Île-aux-Prunes. Downstream this point, the short sediment cores are clearly laminated, and constitute a second subunit of the Champlain Sea Clays. The laboratory analyses point to similar characteristics of all the sediment samples and confirm the presence of the Champlain Sea Clays. The granulometric distribution is dominated by clay and silt, with variable proportions of sand, gravel and pebble. The rare cores dominated by coarse sediments were sampled in dune fields and areas clearly in erosion, where coarse sediments have recently been transported by the strong bottom currents (~ 1 m/s). The carbon and water content of the clays are normal for a marine environment (i.e. total carbon of 0.5 % to 2.3 % and water content of 36.0 ± 5.9 %). In addition, the ^{14}C radiocarbon age obtained from a marine pelecypod shell indicates an age of 11 640 cal BP and the absence of ^{210}Pb in excess is concordant with the erosion trend of the waterway.

Keywords: Boreholes, stratigraphy, sediments, seismic, port, Montreal, *ArcGIS*, multibeam bathymetry, navigation channel, Champlain Sea.

TABLE DES MATIÈRES

REMERCIEMENTS	ix
RÉSUMÉ	xii
ABSTRACT	xiii
TABLE DES MATIÈRES	xv
LISTE DES TABLEAUX	xvi
LISTE DES FIGURES	xvii
LISTE DES ABRÉVIATIONS, DES SYMBOLES ET DES ACRONYMES	xix
INTRODUCTION GÉNÉRALE	1
STRATIGRAPHY AND SEDIMENTARY PROCESSES IN THE WATERWAY OF THE PORT OF MONTREAL	7
1.1 ABSTRACT	7
1.2 INTRODUCTION	9
1.3 GEOLOGICAL AND ENVIRONMENTAL SETTING	10
1.3.1 Study area and hydrology	10
1.3.2 Geology and quaternary sediments	12
1.4 MATERIAL AND METHODS	15
1.4.1 Bathymetry	15
1.4.2 Seismic and coring survey	16
1.4.3 Core analyses	19
1.4.4 Grain size	19
1.4.5 Carbon content	20
1.4.6 Chronology	20

1.4.7	Borehole database	21
1.5	RESULTS	22
1.5.1	Multibeam bathymetry.....	22
1.5.2	Surface sediments	31
1.5.3	Short sediment core.....	33
1.5.4	Chronology	38
1.5.5	Seismo-stratigraphic Units.....	39
1.6	DISCUSSION	44
1.6.1	Chronostratigraphy	44
1.6.2	The erosion trend of the waterway.....	48
1.6.3	Geomorphological features and the sediment composition of the river floor.....	49
1.7	CONCLUSIONS	53
1.8	ACKNOWLEDGMENTS.....	55
	CONCLUSION GÉNÉRALE.....	56
	RÉFÉRENCES BIBLIOGRAPHIQUES.....	62

LISTE DES TABLEAUX

Table 1. Specifications of the instruments used for the CHS bathymetric surveys.....	16
Table 2. Coordinates of the sediment cores used in this study.	18

LISTE DES FIGURES

Figure 1. Navire de recherche F.J. Saucier	Figure 2. Petite carotte sédimentaire.....	4
Figure 3. Location of the sediment cores and the seismic lines acquired during the FJS 2017 expedition on board the R/V F.J. Saucier. The studied area is restricted to the waterway of the Port of Montreal from Montreal to Sorel. The map also illustrates the bathymetry along the location of the collected sediment cores, the location of the two types of cores and the 3 cores having undergone downcore analysis.....	11	
Figure 4. Stratigraphy of the Quaternary successions in the St. Lawrence Lowlands. Modified from (Lamothe and St-Jacques. 2015).....	14	
Figure 5. Gravity corer used in this study on board the R/V F.J. Saucier.	17	
Figure 6. Difference in the bathymetry of the waterway between 2005 and 2017. Red = shallower (accumulation). Blue = deeper (erosion).....	24	
Figure 7. Sensible bathymetry related to the maintained depth for navigation, main dredging marks and fields of migrating dunes.....	25	
Figure 8. a) Bathymetry and b) depth difference from 2005-2014 which illustrate reversed dredging marks with migrating dunes in the center of the waterway. c) Bathymetry and d) depth difference between 2005-2014 illustrating migrating dunes in the center of the waterway and dredging marks north of the waterway. e) Bathymetry and f) depth difference (between 2005 and 2017) showing disappearing dredging marks, a depression in the center of the waterway, and small dunes linearly aligned close to the bottom edge. g) Bathymetry showing dredging marks followed downstream by small dunes in formation nearby the southern-eastern edge of the waterway, and curved sand ribbons and furrows above.	28	
Figure 9. Bathymetry is showing a shallow zone of the waterway partially dredged, then in erosion between a) 2005 and b) 2016. c) Profile 11 shows a mean depth erosion of -0.038 m/yr with a retreat of the head of the form of 24 m upstream. d) Profile # 14 shows a narrowing of the form of 14 m.....	28	

Figure 10. Profile # 30 (plan view represented in figures 6 and 7) showing a field of migrating dunes (1.11 m/yr downstream). The migration is quantified by the migration of the crest between 2005 and 2014.	29
Figure 11. a) Bathymetry of an important accumulation in zone #1 in front of Sainte-Hélène Island and b) difference of bathymetry between 2005-2017 of the same accumulation area. c) South/North profile (#1) indicates a mean accumulation of 0.287 m between 2005-2017 and d) West/East profile (#2) indicates a mean accumulation of 0.184 m for the same period.	29
Figure 12. The sector of accumulation at the tip of Sainte-Hélène's Island. Dunes of different geometries, ribbons and circular forms are creating a sandbank, visible with a) bathymetry and b) the difference in bathymetry between 2005 and 2017.	30
Figure 13. Clay-silt-sand ternary diagram representing the surface samples (0-1 cm) of every core from FJS2017 mission. The core number is indicated for each sample. Core #22 is out of range because it contains a significant amount of gravel. (Modified from GRADISTAT 2001 software.)	32
Figure 14. Carbon contents in surface samples from Montreal to Sorel: total carbon (TC), organic carbon (OC) and inorganic carbon (IC). The space between cores is not representative of the distances. Core # 22 is mainly composed of gravel and sand. No carbon analysis was completed for this core	33
Figure 15. X-ray image and photography of a) unlaminated core with evident OM (FJS2017_27); b) unlaminated core with less OM (FJS2017_15); c) laminated core (FJS2017_03).	34
Figure 16. Clay-silt-sand ternary diagrams of the core FJS2017_03. The box indicates the depth of each sample analysed. The diagram shows the dominance of fine sediments and the relative uniformity of the grain size along the core. (Modified from GRADISTAT 2001 software.)	35
Figure 17. Carbon contents of the cores # 19, 16 and 03: total carbon (TC), organic carbon (OC), and inorganic carbon (IC) contents. Core # 19 contains less carbon than the two others and its values of carbon contents are more constant.	36
Figure 18. Wet bulk density versus "P" wave velocity for each core. A positive correlation is visible between the two parameters. Core #22 is mainly composed of coarse sediments (gravel).....	37

Figure 19. Water content in cores # 19-16-07-03. The water content in the cores # 07-03 show downcore variations unlike cores # 19-16.	37
Figure 20. ^{210}Pb activity for cores # 19-16-07.	38
Figure 21. Quasi-continuous seismic lines from the Jacques-Cartier wharf (Montreal) to the marina of Verchères (lines 0006_298 to 0001_297).	42
Figure 22. (Following figure 21) Quasi-continuous seismic lines from the marina of Verchères to end of the studied area (lines 0001_297 to 0007_297).....	43
Figure 23. Distribution of the bedforms related to the current velocities (shown in cm/s within the circles) and according to Reading (2009): a) general model, b) low sand supply, and c) high sand supply model. Many bedforms of those models are visible in the waterway of the Port of Montreal.	52
Figure 24. Bathymetry of the waterway in the zone of interest #18. See figures 3 and 4 for general location. The black full lines follow the crest of the dunes. The large dunes are usually crescent-shaped. Furrows and ribbons, sand waves and surimposed small dunes cover the riverbed. Picture obtained with the software <i>Caris Hips & Sips</i> (vertical exaggeration of 10:1).....	52

LISTE DES ABRÉVIATIONS, DES SYMBOLES ET DES ACRONYMES

1σ	standard deviation with a confidence interval of 68,27 % / écart-type avec un intervalle de confiance de 68,27% ($2\sigma = 95,45\%$ et $3\sigma = 99,73\%$).
¹⁴C	isotope 14 of carbon / isotope 14 du carbone.
²¹⁰Pb	isotope 210 of lead / isotope 210 du plomb.
cal	calibrated / calibré
C	carbon chemic element / élément chimique carbone.
C_{inorg}	inorganic carbon / carbone inorganique
C_{org}	organic carbon / carbone organique
cc	cube centimeter / centimètre cube
DIC	dissolved inorganic carbon / carbone inorganique dissout
DOC	dissolved organic carbon / carbone organique dissout
dpm	desintegration per minute / désintégration par minute
eV	electron Volt / électron Volt
ft	feet / pied
g	gram / gramme
Hz	Hertz
IC	inorganic carbon / carbone organique

IGLD 85	International Great Lake Datum of 1985 / Système de référence international des Grands Lacs de 1985
inorg	inorganic / inorganique
IRD	Ice Rafted Debris / Débris transporté par les glaces
ISMER	Institut des Sciences de la mer
ka	thousand of years / millier d'années
keV	thousand of electron Volt / miller d'électron Volt
km	kilometer / kilomètre
lbs	pounds / livres
LGM	Last Glacial Maximum / Dernier maximum glaciaire
LIS	Laurentide Ice Sheet / Calotte glaciaire Laurentienne
m	meter / mètre
Ma	million of years / million d'années
MERN	Ministère de l'Énergie et des Ressources Naturelles (Québec)
ms	millisecond / milliseconde
MSCL	Multi-Sensor Core Logger
MSL	Mean Sea Level / Niveau moyen de la mer
N	nitrogen chemic element / élément chimique azote
OC	organic carbon / carbone organique
OM	organic matter / matière organique

org	organic / organique
Pa	Pascal (Newton/m ²)
Pb	lead chemic element / element chimique plomb
PIC	particular inorganic carbon / carbone inorganique particulaire
POC	particular organic carbon / carbone organique particulaire
POM	particular organic matter / matière organique particulaire
ppm	part per million
Ra	radon chemic element / element chimique radon
s	second / seconde
SD	standard deviation / deviation standard
SR	sedimentation rate / taux de sédimentation
T^{1/2}	half-time life / temps de demi-vie
TC	total carbon / carbone totale
tot	total / total
TWT	Two Way Travel time / temps d'aller-retour de l'onde sismique
µm	micro-meter / micro-mètre
WC	water content / teneur en eau
Yr	year / année

INTRODUCTION GÉNÉRALE

Mise en contexte du projet

L'étude des écosystèmes hydriques occupe une place grandissante dans le contexte actuel des changements climatiques et dans la quantification des changements dus aux activités anthropiques. Les océans, les fleuves, les rivières et les autres cours d'eau sont en effet directement influencés par les changements naturels ou anthropiques comme le démontre le rapport du Groupe d'experts intergouvernemental sur l'évolution du climat (Intergovernmental Panel on Climate Change et al., 2014). Le fleuve Saint-Laurent fait l'objet de plusieurs études (p.ex. Painchaud et Villeneuve, 2003; Société de développement économique du Saint-Laurent, 2013), car il occupe une place primordiale dans la structure socioéconomique de l'Amérique du Nord. Le fleuve Saint-Laurent, combiné aux Grands Lacs, forme l'une des plus longues voies navigables commerciales du monde, mesurant plus de 3000 km (The Royal Canadian Geographical Society, 2019). Cette voie navigable est contrôlée et exploitée par les industries maritimes en partenariat avec le gouvernement. C'est par exemple le cas du Port de Montréal. Ce dernier est situé à 1600 km de l'océan Atlantique dans l'est du Canada. Cet emplacement est stratégique par son accès direct et économique aux principaux marchés du centre du Canada, ainsi que du Nord-est comme celui du *Midwest* des États-Unis. Au cours des cinq dernières années, une moyenne annuelle de plus de 30 millions de tonnes de marchandises a transigé par le port, tandis que 2 738 navires ont accosté à Montréal en 2018 (Montreal Port Authority, 2019). Les travaux de dragage, la nature des sédiments, les contaminants, les variations du débit du fleuve, la qualité de l'eau et plusieurs autres paramètres doivent être pris en compte afin de comprendre les changements que subit le Saint-Laurent en réponse à ces activités commerciales (Pelletier, 2005; Talbot, 2006; Tougas-Tellier et al., 2013).

L'ensemble des terres du Québec est plutôt bien caractérisé par des études scientifiques décrivant la nature des sols et du socle rocheux (Brouard et al. 2016; Lamothe and St-Jacques, 2015; LaSalle, 1963; Gouvernement du Québec, 2019). Cependant, la stratigraphie du fleuve Saint-Laurent dans sa portion fluviale, et particulièrement dans le chenal de navigation, est encore méconnue. Produire une étude moderne de la géologie sédimentaire du chenal de navigation entre Montréal et Sorel-Tracy constitue donc le fondement de mon projet de maîtrise. Le Port de Montréal vise en effet à optimiser la compréhension du phénomène d'accumulation de sédiments dans les voies navigables du Saint-Laurent. Le but est de garder une compétitivité internationale, en augmentant l'efficacité des opérations de dragage menées annuellement. Le présent travail est la première étape d'un projet de grande envergure qui aboutirait potentiellement en l'approfondissement du chenal de navigation.

Les objectifs de la recherche

Le principal objectif de ce projet de maîtrise est de caractériser les sédiments, la stratigraphie et les changements sédimentologiques agissant dans les eaux navigables du chenal de navigation entre Montréal et Sorel-Tracy. Pour ce faire, la première étape du projet a été un stage que j'ai effectué à l'administration du Port de Montréal à l'été 2016. Ce stage était une entente entre le Port de Montréal, l'Université du Québec à Rimouski et l'Université du Québec à Chicoutimi. Le résultat principal de ce stage est la structuration et le peuplement d'une base de données géoréférencée *ArcGis* regroupant les informations géotechniques sur le chenal de navigation du Saint-Laurent (principalement des descriptions de forages). Ensuite, des données pluriannuelles de bathymétrie multifaisceaux fournit par le Service Hydrographique du Canada (SHC) permettent d'interpréter les processus sédimentaires dans la voie navigable et d'identifier les zones d'intérêt propices à un suivi annuel de la sédimentation. Des données de sismique réflexion, de multiples analyses en laboratoire de petites carottes sédimentaires, ainsi que la base de données

ArcGIS permettent finalement d'identifier les principales unités sédimentaires et d'établir la stratigraphie le long du chenal de navigation.

Mission d'échantillonnage

La mission FJS2017 avait pour but premier d'acquérir des données géologiques complémentaires à celles de la base de données *ArcGIS* initiale, en plus des levés de multifaisceaux fournis par le SHC. La mission scientifique effectuée à bord de la vedette hydrographique F.J.-Saucier (Fig. 1) du Centre interdisciplinaire de développement en cartographie des océans (CIDCO) a permis d'acquérir des carottes sédimentaires (Fig. 2), des échantillons de sédiments de surface et de faire des levés sismiques. La zone d'étude s'étend de Montréal (quai Jacques-Cartier) jusqu'à Sorel-Tracy (limite des eaux navigables du Port de Montréal) et se concentre sur le chenal de navigation en tant que tel. Cette zone fait 65 km linéaires sur 250 m de largeur et touche 12 municipalités différentes (Fig. 3).

Le chenal de navigation est constamment actif et parcouru par une moyenne de 40 à 50 navires/jour (François, 2015), en plus d'avoir une forte vitesse du courant. Ces paramètres ont conduit à l'utilisation d'un profileur de sous surface (CHIRP) de marque *Knudsen* (modèle 3212 à 3,5 kHz) pour réaliser les levés de sismique, ainsi qu'à la modification d'un carottier *WILDCO* à gravité (Fig. 5) pour récolter des carottes sédimentaires. D'ailleurs, certaines zones soupçonnées plus agitées et géologiquement plus compactes et/ou à sédiments grossiers, n'ont pas pu être échantillonnées avec le carottier. Quatre jours sur l'eau ont permis d'obtenir 148 km linéaires de levés sismiques et 27 petites carottes sédimentaires.



Figure 1. Navire de recherche F.J. Saucier
(source CIDCO)



Figure 2. Petite carotte sédimentaire

Organisation du mémoire et contribution

Ce mémoire de maîtrise est présenté sous la forme d'un article scientifique rédigé en anglais. L'article devrait être soumis dans les mois à venir à une revue scientifique telle que *Sedimentology*.

En raison de l'ampleur du projet et ses multiples aspects techniques, plusieurs personnes-ressources ont contribué en apportant des conseils en informatique et en effectuant des analyses en laboratoire. Marie-Pier St-Onge a effectué les analyses de granulométrie laser sur la partie fine des échantillons des petites carottes sédimentaires. Quentin Beauvais a effectué les analyses des carottes au MSCL et il a ajusté les coordonnées géographiques des levés de sismique. La datation au ^{14}C a été réalisée par le laboratoire *BETA Analytic* en Floride. Les mesures des isotopes du ^{210}Pb ont été faites par Claude Rouleau et Pascal Rioux à la station aquicole de Rimouski. Mathieu Babin et Marie-Ève Anglehart ont effectué les analyses des teneurs en carbone au spectromètre de masse. J'ai pour ma part échantillonné et préparé les échantillons pour toutes ces analyses.

(ouverture des carottes, échantillonnage, tamisage, préparation au Calgon, acidification, teneur en eau, séchage, encapsulage, emballage avec de la paraffine, etc.). J'ai par la suite compilé, analysé et présenté les résultats.

Par ailleurs, j'ai organisé et supervisé la mission FJS2017 avec le soutien de Guillaume St-Onge, Patrick Lajeunesse, Quentin Beauvais et Sylvain Gauthier. J'ai ensuite effectué l'analyse des données de sismique réflexion sur le logiciel *Kingdom*, ainsi que l'analyse et le traitement des données de bathymétrie multifaisceaux sur les deux logiciels *Caris Hips & Sips* et *ArcGIS*.

Guillaume St-Onge m'a apporté aide et conseils tout au long de mon projet. Il a lu, corrigé et amélioré mes présentations orales, mes affiches scientifiques, mes résumés, mes rapports de stage/mission et mon mémoire de maîtrise plusieurs fois au cours de ces trois années au cycle supérieur.

Présentations officielles lors de congrès

Le stage que j'ai effectué au Port de Montréal l'été avant de commencer ma maîtrise est présenté dans un rapport soumis à l'Université du Québec à Chicoutimi. Ce rapport constitue la première présentation officielle sur mon projet. Tout au long de la maîtrise, j'ai ensuite participé à plusieurs missions, congrès, rencontres et conférences. J'ai produit et présenté des affiches scientifiques et des présentations orales sous forme de conférence. Voici la liste de mes présentations et contributions :

Nadeau, S. 2016. Stage en géomatique et géotechnique au Port de Montréal. Rapport de stage effectué à la fin du baccalauréat en génie géologique, mai-août 2016, Administration du Port de Montréal, Montréal (Qc), Canada

Nadeau, S., St-Onge, G., Dumontier, L. 2017. Stratigraphie et processus sédimentaires dans le Port de Montréal et sa voie navigable. Affiche et résumé lors du congrès du GEOTOP 2017. 24-26 mars 2017, Forêt Montmorency (Qc), Canada

Nadeau, S. 2017. À la limite de la nordicité canadienne. Présentation de la mission scientifique sur l'Île d'Ellesmere à laquelle j'ai participé du 20 mai au 7 juin 2017 sur l'Île d'Ellesmere, Canada. Présentée lors d'un midi-conférence, ISMER

Nadeau, S., Desiage, P.-A., Beauvais, Q., Trottier, A.-P., St-Onge, G., St-Pierre, A. 2017. Mission scientifique FJS2017 : Chenal de navigation du Saint-Laurent entre Montréal et Sorel-Tracy à bord du N/R F.J. Saucier. 23 au 28 octobre 2017, Verchères (Qc), Canada. Rapport de mission produit par Simon Nadeau pour l'UQAR

Nadeau, S., St-Onge G., 2018. Stratigraphie et processus sédimentaires dans le Port de Montréal et sa voie navigable. Présentation du déroulement du projet de maîtrise devant les dirigeants du Port de Montréal. 15 février 2018, Montréal (Qc), Canada

Nadeau, S., St-Onge, G., Dumontier, L. 2018. First characterization of the stratigraphy and sedimentary processes in the waterway of the Port of Montreal in a perspective of optimizing no destructive data acquisition. Affiche et résumé lors du congrès du GEOTOP 2018. 21-23 mars 2018, La Malbaie (Qc), Canada

Nadeau, S., St-Onge, G., Dumontier, L., Lajeunesse, P. 2018. First characterization of the stratigraphy and sedimentary processes in the waterway of the Port of Montreal. Conférence et résumé lors de l'International Sedimentological Congress, 26 juin au 6 juillet 2018, Québec (Qc), Canada

STRATIGRAPHY AND SEDIMENTARY PROCESSES IN THE WATERWAY OF THE PORT OF MONTREAL

Simon Nadeau^{1} and Guillaume St-Onge¹*

* Corresponding author

¹ Canada Research Chair in Marine Geology, Institut des sciences de la mer de Rimouski (ISMER), Université du Québec à Rimouski

1.1 ABSTRACT

A good understanding of the stratigraphy and the sedimentary processes are required to ensure the security of maritime transport and dredging operations around an international port. A research project was thus established to characterize the sediments, their composition and stratigraphy, and the sedimentary processes acting in the Port of Montreal and its waterway. A geodatabase was firstly developed from the geotechnical archives of the Port of Montreal and its partners. It integrates thousands of borehole descriptions recorded since 1830 AD. A sampling mission was then realised on board the scientific vessel F.J. Saucier. It resulted in the acquisition of 148 km of acoustic subbottom profiles (3.5 kHz) and 27 short sediment cores. The analysis of multiannual bathymetric multibeam echosounding data provided by the Canadian Hydrographic Service shows that a mean erosion trend of 2.7 cm/yr is occurring in the waterway since the last 12 years. The shapes and migration rates of subaqueous dunes and other submarine features also denote a low-supply sediment model. However, the area between the Jacques-Cartier wharf and the end of the Boucherville's Island is subject to accumulation (up to 14 cm/yr) and needs to be closely monitored. The seismic data combined to the *ArcGIS* borehole descriptions and the short sedimentary cores indicate outcropping of the bedrock (Shale of Utica) in this sensible area. The bedrock then plunges in front of the Ste-Thérèse Island and the Quaternary overlying sediments outcrop with an unlaminated subunit of the Champlain Sea Clays until a threshold in front of the Île-aux-Prunes. Downstream this point, the short sediment cores are clearly laminated, and constitute a second subunit of the Champlain Sea Clays. The laboratory analyses point to similar characteristics of all the sediment samples and confirm the presence of the Champlain Sea Clays. The granulometric distribution is dominated by clay and silt, with variable proportions of sand, gravel and pebble. The rare cores dominated by coarse sediments were sampled in dune fields and areas clearly in erosion, where coarse sediments have recently been transported by the strong bottom currents (~1 m/s). The carbon and water content of the clays are normal for a marine

environment (i.e. total carbon of 0.5 % to 2.3 % and water content of 36.0 ± 5.9 %). In addition, the ^{14}C radiocarbon age obtained from a marine pelecypod shell indicates an age of 11 640 cal BP and the absence of ^{210}Pb in excess is concordant with the erosion trend of the waterway.

Keywords: Boreholes, stratigraphy, sediments, seismic, port, Montreal, *ArcGIS*, multibeam bathymetry, navigation channel, Champlain Sea.

1.2 INTRODUCTION

The St. Lawrence River and the Great Lakes constitute one of the longest commercial waterways in the world with more than 3000 km (The Royal Canadian Geographical Society 2019). The Port of Montreal is located 1600 km from the Atlantic Ocean in Eastern Canada. This location is strategic by its direct and economic access to major markets in Central Canada, likewise the Northeast and the Midwest of the USA. In the last 5 years, more than 30 million tons of merchandise per year were handled in the port, while 2738 ships docked in Montreal in 2018 (Montreal Port Authority, 2019). A good understanding of the stratigraphy and the sedimentary processes is thus required to ensure the security of the maritime transport and dredging operations around this international port. The Quaternary geology of St. Lawrence Lowlands was described by many studies (e.g. Brouard et al. 2016; Carrier et al., 2013; Dubé-Loubert et al., 2014; Lamothe and St-Jacques, 2015; LaSalle, 1963). These studies partially characterise the banks of the St. Lawrence River, including their sensitivity to erosion (Gaskin et al., 2003), but an understanding of the sedimentary processes on the riverbed of the waterway and its stratigraphy are still missing. This project was thus established to characterize the sediments, their stratigraphy, and the sedimentary processes acting in the Port of Montreal and its waterway. In this paper, pluriannual multibeam bathymetric data will be presented and interpreted to better understand the sedimentary processes in the waterway, areas of interest that are propitious to an annual monitoring of the sedimentation will be identified, and seismic data, sediment core analysis and available borehole data will be combined to establish the main stratigraphic units along the navigation channel.

1.3 GEOLOGICAL AND ENVIRONMENTAL SETTING

1.3.1 Study area and hydrology

The studied area of the present paper is limited to the waterway between the Jacques-Cartier wharf in Montreal and the limit of the navigable waters under the jurisdiction of the Port of Montreal, which is close to Sorel-Tracy (Fig. 3). The width of the waterway is 250 m and the studied portion is 65 km long. This fluvial portion of the St. Lawrence was dug in the last 100 years (Baillargeon, 2015) and is dredged every year to ensure a minimal depth of 11.3 m. The studied portion of the St. Lawrence river has no stratification of the water column, flows around 1 m/s (Leclerc et al., 1991) and is not affected by the tide (Godin, 1999). The occupation of the lands surrounding the studied area is mostly dominated by farming lands, residential and commercial constructions (Lamontagne et al. 2000).

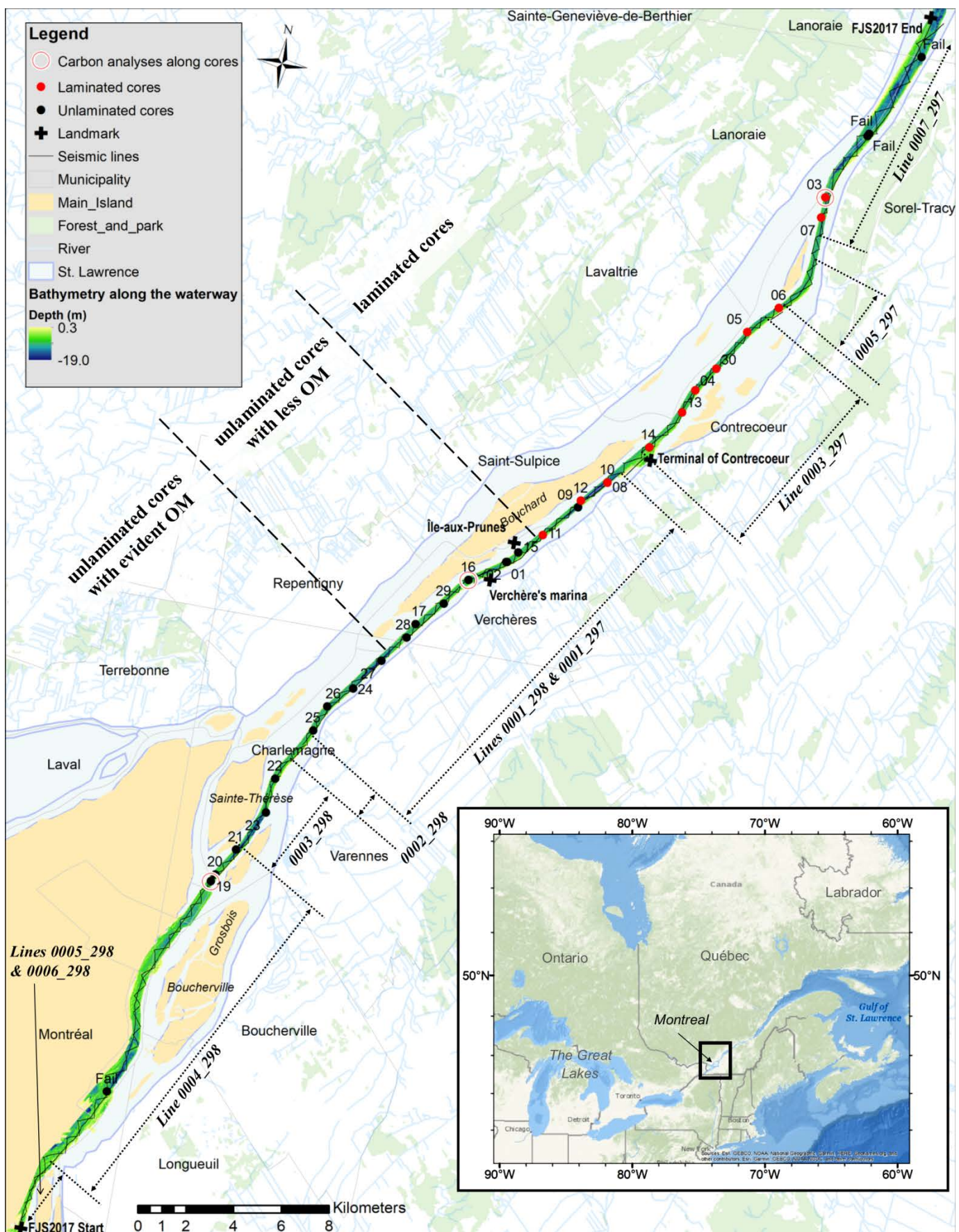


Figure 3. Location of the sediment cores and the seismic lines acquired during the FJS 2017 expedition on board the R/V F.J. Saucier. The studied area is restricted to the waterway of the Port of Montreal from Montreal to Sorel. The map also illustrates the bathymetry along the location of the collected sediment cores, the location of the two types of cores and the 3 cores having undergone downcore analysis.

The Great Lakes St. Lawrence water system is complex to characterize due to the human activities that affect the water level, the inputs of many tributaries, the effect of islands and lakes, the balance of the water cycle on a large area and other specific local features. Reporting the flow at Sorel is therefore a common practice because it simplifies the estimations of the rate of flow. Between 1932 and 2012, the flow varied from 6 000 m³/s to 20 000 m³/s (Government of Canada, 2019). The regulation of the water level greatly influences the mean monthly flow, so annual compilation is used for monitoring. The mean annual flow is usually around 8000-11 000 m³/s and the main two tributaries are the Ottawa River (1000 to 8000 m³/s) and the Great Lakes (6000 to 9000 m³/s) (Bouchard and Cantin, 2015). A distinction has to be made between the whole river and the navigation channel (the waterway) because the hydrologic conditions are quite different. In fact, Dolgopolova and Isupova (2011) indicated that the sedimentation in the river portion of the St. Lawrence is located beyond the waterway, where the bathymetry is low (around 4.5 m) and the current is not greater than 0.3 m/s. They also observed that the suspended sediment concentration varies between 4 to 10 mg/l in the portion studied. According to Rondeau et al. (2000), the annual sediment load at the end of the studied area cumulate 28×10^5 t/yr. From this suspended sediments, the particulate organic carbon (POC) originated from a mixture of terrestrial and aquatic production with seasonal variations, and represents 0.1 to 0.13×10^{12} g every year at its arrival in the estuary. The dissolved organic carbon (DOC) is ten time more abundant than the POC and mostly originated from terrestrial production all year round (Hélie, 2004).

1.3.2 Geology and quaternary sediments

The studied area is located in the autochthonous domain of the St. Lawrence Platform. The Platform is bordered at the north-west by the Grenvillian geologic province and at the south-east by the Appalachians. The St. Lawrence Platform consists in sedimentary rocks of Cambrian to Ordovician ages (542 - 444 Ma), disposed in horizontal strata that disconformably overlie the Grenvillian basement rocks (Precambrian). In

stratigraphic order, the geological groups that form the St. Lawrence Platform are named: Postdam, Beekmantown, Chazy, Black River, Trenton, Shales of Utica, Sainte-Rosalie, Lorraine, and Queeston formations (Carrier et al., 2013; Globensky, 1987). The subsurface geology of the area covered in this paper is mapped by the "Ministère de l'Énergie et des Ressources Naturelles" (MERN) of Québec and by Thériault (2012). It presents the outcrop of two geological groups: the Shales of Utica and the Lorraine Group (Nicolet and Pontgravé formations). Those rocks have been deposited during the Upper Ordovician. The shale of Utica is calcareous and was deposited in deep water conditions during a marine maximum. The rock formations of Nicolet and Pontgravé consist of interstratified shale, sandstone, siltstone and limestone. Séjourné et al. (2002) demonstrated that the sedimentary rocks were affected by syn-sedimentary normal faults reactivated during the Late Ordovician Taconic Orogeny. The Taconian Orogeny also created the thrust sheets (i.e. the allochthons) that overlap the south-west part of the St. Lawrence Platform. The Logan Fault determinates the limit between the autochthonous/parautochthonous and the allochthonous domains (constituted of Humber and Dunnage zones). This stratigraphy is the result of the opening and the closure of the Iapetus ocean basin.

The Quaternary period in the St. Lawrence Lowlands is marked by a succession of three major advances/retreats of the Laurentian Ice Sheet (LIS) (Carrier et al., 2013). The oldest glacial unit known is the "Bécancour Till", which resulted from the Illinoian Glaciation (> 130 ka, (Bourque, 2004)). Then, the Sangamonian interglacial (130 to 80 ka) allowed the deposit of glaciolacustrine rhythmites (Fig. 4) until the second glacial advance. The "Deschaillons Varves" and the "Lévrard Till" testify the glacial re-advance that occurred during the Lower Wisconsinan (75 to 65 ka) (Dubé-Loubert et al., 2014). The "La Pérade Clay" represents a short marine episode between this last glacial event and the following interglacial episode (Ferland and Occhietti, 1990). The interglacial episode of the Middle Wisconsinan (65 to 23 ka) is represented by the "St. Pierre Sediments" (fluvial and glaciolacustrine sediments). The Last Glacial Maximum (LGM) occurred around 18 500 ka during the Upper Wisconsinan. The "Gentilly Till" is a deposit characteristic of the LGM in

the St. Lawrence Lowlands. Prest et al. (1982) separated this deposit in two part for the Montreal region : Malone Till and Fort Covington Till.

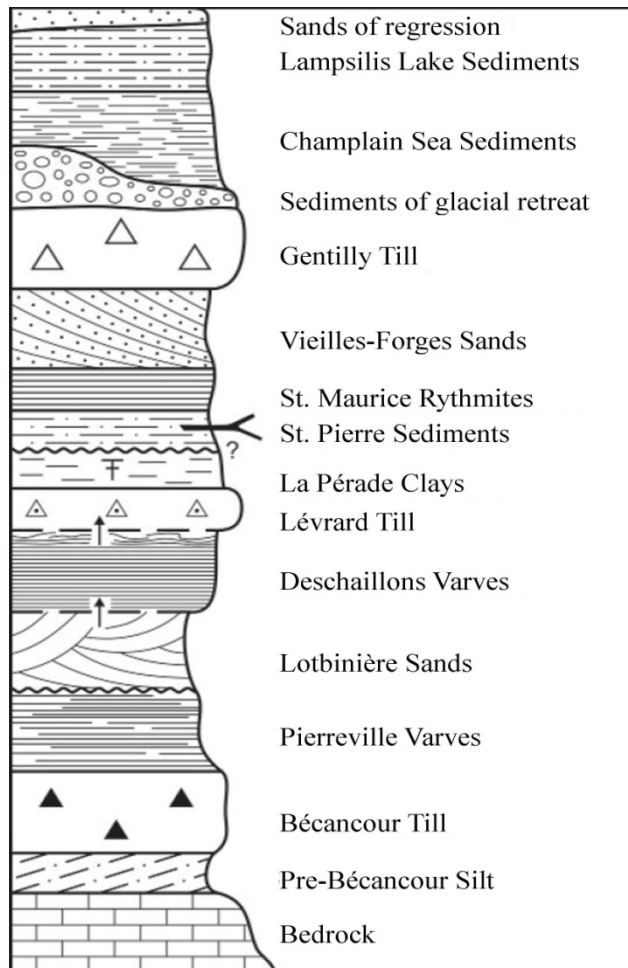


Figure 4. Stratigraphy of the Quaternary successions in the St. Lawrence Lowlands.
Modified from (Lamothe and St-Jacques. 2015).

At the end of the Pleistocene (12 000 - 10 000 yr), the gradual ice retreat of the LIS had created eskers, moraines, kames and other fluvio-glacial deposits. The marine invasion of the Champlain Sea occurred simultaneously ($\sim 11\ 200$ yr) to the ice retreat. It resulted in the silty-clayey marine deposits called the "Champlain Sea Clay" (Occhietti et al., 2001). This embayment was then isolated from the Atlantic Ocean by the isostatic rebound and as a result, created the fresh water Lampsilis Lake around 9800 yr (Carrier et al., 2013). The

marine limit reached the elevation of 183 m (Gadd, 1971) while marine sediment were found under the elevation of 175 m (Lamothe and St-Jacques, 2015).

The sediments of the present study were sampled in the waterway and were located at a negative elevation according to the International Great Lakes Datum of 1985 (IGLD85).

1.4 MATERIAL AND METHODS

1.4.1 Bathymetry

The bathymetric data used in this study was acquired by the CHS over many years, compiled from three different research vessels with a spatial grid between 0.25 and 2.5 m depending on the available data: the *CCGS Morillon*, *F.C.G Smith*, and *GC-03*. The specifications of the systems used on each vessel are presented in table 1. Data was combined by the CHS to create annual bathymetric surfaces from 2005 to 2017. The CHS provides a vertical accuracy of 20 cm and less for those data. The initial data processing was performed by the CHS to produce bathymetric layers, saved as «.csar» format (x,y,z). The software *Caris Hips & Sips* was then used to spatially and temporally visualize the data and thus geomorphological changes. Exported from *Caris* to *ArcMap*, zones of interest have then been investigated at the maximum grid resolution available (often: ± 0.5 m) by three visualization technics: depth difference between years, bathymetric color map with hillshade, and bathymetric color map classified by the water depth critical for navigation. The spatial availability of data over the years (coverage % calculated with *ArcGIS* tools) was the major element influencing the delimitation of the zones of interest. The bathymetric survey of 2017 covers 65.5% of the waterway. The blanks have been filled with previous bathymetric data of 2016 and 2012 to calculate the general sedimentation over 13 years. Less than 10% of the data come from 2012. Nevertheless, the annual sedimentation was calculated in areas with full data coverage. Comparison of profiles and statistics of bathymetric changes were then used to quantify the dunes, the sedimentary regime, and other geomorphological features. The accumulation and erosion rates given in

the results represent a mean of the calculations operated cell by cell on annual bathymetric data.

Table 1. Specifications of the instruments used for the CHS bathymetric surveys

Year	Vessel	Positioning	Attitude	Echosounder	Frequency
2005 -2018	F.G.C. Smith	Aquarius (Magellan) and Proflex800 (SpectraPrecision)	Orion INS (Teledyne)	Multi-transducers (Navitronic) 33 transducers	200 kHz
2005 -2013	GC-03	Aquarius (Magellan) and Proflex800 (SpectraPrecision)	Orion INS (Teledyne)	Multi-transducers (Navitronic) 12 transducers	200 kHz
2014 -2018	GC-03	Proflex800 (SpectraPrecision)	PosMV OceanMaster (Applanix)	Multi-beam EM2040D (Kongsberg)	300 kHz
2005 -2012	Morillon	Aquarius (Magellan) and Proflex800 (SpectraPrecision)	HMR3000 (HoneyWell)	Multi-transducers (Navitronic) 6 transducers	200 kHz
2013 -2018	Morillon	Proflex800 (SpectraPrecision)	PosMV OceanMaster (Applanix)	Multi-beam Sonic2020 (R2Sonic)	300-400 kHz

The accuracy of those instruments varies with the mode used to obtain the data.

Aquarius: horizontal = 5 to 200 mm, vertical = 10 to 200 mm

Proflex800: horizontal = 10 to 100 mm, vertical = 20 to 200 mm

PosMV: position = 8 to 100 mm 95%, heave = 2 to 5 cm

Orion INS: heading = 0.1°, heave = 5 cm ± 1 cm

HMR3000: heading = 0.5 to 1.5 °RMS ± 1.0°

1.4.2 Seismic and coring survey

The FJS2017 expedition was carried on board the research vessel F.J.-Saucier, a 7.9 m-long *Cheetah* Marine Catamarans of the Centre Interdisciplinaire de Développement en Cartographie des Océans (CIDCO) from October 24 to 27, 2017. The seismic survey covered the waterway from Montreal to the limit of the navigable water under the jurisdiction of the Port of Montreal, which is close to Sorel (Fig. 3). The coring sites are also located throughout this area.

148 km of seismic data was acquired using a *Knudsen* 3.5 kHz (model 3212) sub-bottom profiler (CHIRP). This instrument allows penetration of the acoustic waves between 0 to 100 m depending on the sediment's nature and the vertical resolution is around 1-15 cm in the actual environment according to the maker. The software of the *Knudsen* instrument automatically processes the data by applying a time-variant gain (TVG) (Schock et al., 1989) and outputs data in «.keb» and «.sgy» formats. The *Kingdom Suite®* software was then used to interpret the seismic data and pick the acoustic reflections. The sound velocities assumed for the conversion from Two Way Travel time (TWT) to depth are 1450 m/s in the water column and 1600 m/s in the sediments. This is in agreement with the sediment velocity results performed on the short sedimentary cores (see below). The depths are given in relation to the water level during the FJS2017 expedition, which was on average 0.72 m above the Chart Datum IGLD 1985.

Coring was performed with a modified WILDCO® gravity corer (Model 2416-B45 *BallchekTM*, (Fig. 5), on which an extra weight of 40 lbs was added to reduce the effect of currents. The diameter of the 27 short sediment cores is 2 inches and the lengths vary between 10 and 36 cm (Table 2).



Figure 5. Gravity corer used in this study on board the R/V F.J. Saucier.

Table 2. Coordinates of the sediment cores used in this study.

Station	Length (cm)	WGS_1984_UTM_Zone_18N		
		Coord_X	Coord_Y	Description
FJS2017_01	----	628264	5071615	No core, only sediment trapped in the core catcher
FJS2017_02	25	628302	5071622	Core + sediment trapped in the core catcher
FJS2017_03	28,5	638447	5089154	Core
Station not sampled	----	641277	5095686	No sample
FJS2017_04	24	634659	5080186	Core + sediment trapped in the core catcher
FJS2017_05	21	636328	5083001	Core
FJS2017_06	20	637428	5084242	Core + sediment trapped in the core catcher
FJS2017_07	17	638437	5088287	Core + sediment trapped in the core catcher
FJS2017_08	12	631788	5075685	Core
FJS2017_09	----	630784	5074432	Bag
FJS2017_10	18	631783	5075696	Core
FJS2017_11	18	629556	5073022	Core + sediment trapped in the core catcher
FJS2017_12	17,5	630844	5074733	Core
FJS2017_13	21	634288	5079173	Core
FJS2017_14	24	633224	5077476	Core + sediment trapped in the core catcher
FJS2017_15	17	628687	5072108	Core
FJS2017_16	22	626860	5070581	Core + sediment trapped in the core catcher
FJS2017_17	10	625044	5068332	Core
FSJ2017_18	----	616105	5046672	No sample, broken core catcher
FSJ2017_19	36	618689	5056130	Core + sediment trapped in the core catcher
FSJ2017_20	28,5	618822	5056451	Core
FSJ2017_21	19	619477	5057635	Core
FSJ2017_22	13	620516	5060861	Core + sediment trapped in the core catcher
FSJ2017_23	23	620401	5059392	Core + sediment trapped in the core catcher
FJS2017_24	17,5	622990	5065190	Core + sediment trapped in the core catcher
FSJ2017_25	30	621690	5063146	Core
FSJ2017_26	23	622066	5064244	Core + sediment trapped in the core catcher
FSJ2017_27	15,5	623932	5066554	Core
FSJ2017_28	22	624775	5067708	Core
FSJ2017_29	21	626035	5069408	Core
FSJ2017_30	26	635347	5081244	Core
FJS2017_31	----	639699	5092015	No sample, broken core catcher
Station not sampled	----	639746	5092118	No sample

1.4.3 Core analyses

The cores were first passed through a *GEOTEK XCT* scanner at the Institut des sciences de la mer de Rimouski (ISMER) to visualize the sedimentary structures and to derive a density profile from the acquired digital X-ray images (Fortin et al., 2013; St-Onge and Long, 2009). The physical properties of the whole cores were then analyzed with a *GEOTEK Multi-Sensor Core Logger (MSCL)* at ISMER (St-Onge et al., 2007). Wet bulk density, «P» wave velocity and magnetic susceptibility were all measured at 0.5 cm intervals. The cores were then split, photographed, described and magnetic susceptibility was measured again at 0.5 cm on the split cores using a point source sensor. In addition, diffused spectral reflectance was measured with a *Konica Minolta CM-2600d spectrophotometer* and the chemical composition was determined with an *Olympus InnovXsystem X-Ray fluorescence spectrometer* online with the MSCL.

1.4.4 Grain size

The sediments were first sieved at 2 mm to facilitate the subsequent analyses. The weight and dimensions of the outlier gravel and cobbles were measured manually. Due to the combined presence of sand, fine clay and coarse silt, a second step of sieving was necessary at 63 µm before further analyses. The sediments coarser than 63 µm constitute the sequence one. The sediments finer than 63 µm form the second sequence, which was diluted into a solution of Calgon for at least 24 hours before being analyzed. Those steps were made for each surface sample and for each centimeter of core FJS2017_03. The grain size distributions of the two sequences were determined using a *Beckman Coulter LS13320* laser sizer. The two last runs of each sample were averaged to obtain reliable data. The grain-size distribution data were then combined and processed with the *GRADISTAT* software (Blott and Pye, 2001) to obtain the statistical parameters of the sediments.

1.4.5 Carbon content

The surface (0-1 cm) of each sediment core and cores # 03, 16 and 19 (sampled at 1 cm intervals) were sampled for carbon content. The measurements were performed with a *Costech™* model 4010 elemental analyzer coupled to a mass spectrometer *Deltaplus XP* from *ThermoScientific*. Ten standards from the National Institute of Standards and Technology (NIST) are used for each sequence of analysis (36 samples or less) to calibrate the sample results via a linear correction. The quantification was based on an external secondary standard with a calibration range of 0.040 to 0.400 mg for carbon. All samples were separated into two aliquots. One aliquot was directly dried and analyzed for its total carbon content (TC), while the other was acidified four times with HCl (12 M) to dissolve carbonates, then dried and finally analyzed. The acidified replicates are assumed to represent the organic carbon content (OC). The inorganic carbon content is calculated by subtracting the OC from the TC contents. Uncertainty, as determined from the analysis of standard materials is $\pm 4\%$ (relative).

1.4.6 Chronology

Core FJS2017_16 has been sampled every centimeter to measure ^{210}Pb activity. Prior to analysis, samples were dried, crushed, and confined into polyethylene containers of cylindrical geometry filled in with paraffin and sealed with Teflon tape, according to the method described by Cutshall et al. (1983) and San Miguel et al. (2002). Samples then rested at least 2 weeks to reach the secular equilibrium ($^{226}\text{Ra}/^{210}\text{Pb}$). Direct analysis of ^{210}Pb by gamma-ray spectrometry was performed with the *ORTEC* coaxial photon detector system: a High-Purity Germanium detector (Gamma-X HPGe) model GMX50-S, with 56.3% of relative efficiency (measured) at 1330 keV, and full-width at half-maximum (FWHM) of 2.11 keV at 1330 keV and 0.705 keV at 5.9 keV. The measurements were performed at the underground laboratory of ISMER at its aquaculture station. The data was processed with the *GammaVision* software, (version 6.06) which was used to quantify and

correct the energy peaks of the ^{210}Pb (46.52 keV). In the three measured cores, no radioactive decay was observed.

The radiocarbon conventional age ($10\,880 \pm 40$ yr BP) of a marine pelecypod shell sampled in core FJS2017_16 at 7-8 cm was determined with an accelerator mass spectrometer at *Beta Analytic Laboratory* (Laboratory #: Beta - 496132). The age 11 640 cal BP (min: 11 360 cal BP, max: 11 880 cal BP, 2σ) was calibrated with the *CALIB 7.1.0* online software using the MARINE13 datasets (Reimer et al., 2016). A marine reservoir correction of -800 years ($\Delta R = 400$) was used for the calibration because the age falls within the Younger Dryas when the thermohaline circulation was weaker (Bard et al., 1994; St-Onge et al., 2008).

1.4.7 Borehole database

The *ArcGIS* borehole geodatabase was constructed from the geotechnical archives of the Port of Montreal and its partners. Several data processing and correction steps were applied to integrate borehole descriptions from relatively old (up to 1830 AD) and more recent studies. The majority of the boreholes have a relatively poor geospatial precision (radius of $\pm 50\text{-}100$ m around « x,y » coordinates) due to the transfer of information from meter-long paper maps or the absence of effective positioning during drilling. The location of the boreholes is consequently not used to validate the depth values of the seismic reflections, but rather for the description of each sedimentary sequence and their respective thickness, which are useful to interpret the seismic data.

1.5 RESULTS

1.5.1 Multibeam bathymetry

The width and the length of the navigation channel (250 m x 65 km) make it difficult to represent geomorphological features and their changes in one continuous figure. Hence, we separated the entire area in 20 zones. Ten main zones of interest were then selected according to the availability of bathymetric information over the years. The zones # 1-4-5-6-9-10-12-14-17-18 shown in figures 6 and 7 contain enough bathymetric data (spatially and temporally) to study subaqueous forms on representative and selected areas.

The depth water varies between 6.67 and 19.29 m from Montreal to Sorel. The overall depth difference in the waterway between 2005 and 2017 indicates a slight trend for erosion of 0.027 m/yr. The portions of the waterway being in erosion seem on average more frequent than portions being in accumulation (Fig. 6).

An exception to this trend occurs from Jacques-Cartier wharf to the end of Boucherville's islands (zones of interest 1, 4 and 5, Fig. 6). In addition, the accumulation occurs every year, particularly in zone 1, when looking at these zones year after year. Furthermore, the water depth of this area is near or below the objectives of the Port of Montreal (Fig. 7), which is to maintain a depth of 11.3 m. The main zone of interest #1 is characterized by constant accumulations in two sectors: 1) between Sainte-Hélène's Island and Montreal's Island (Figs. 2 and 11) at the tip of Sainte-Hélène's Island (Fig. 12). Between 2005 and 2017, the first sector has a mean accumulation rate of 0.024 m/yr, but it varies from an erosion of 0.012 m between 2005 and 2006, to an accumulation of 0.141 m/yr between 2011 and 2013, and finally no change (0.008 m) between 2016 and 2017. Similar variations in sedimentation accumulation are observable along and across the waterway in the first sector. Despite the precision of the data, this sector is subject to dredging works and the erosion or no change results could underestimate the real accumulations. The trend to accumulation for this sector is consequently the main valid result.

Another exception to the general erosional trend appeared between 2007 and 2008, where a mean accumulation of 0.039 m/yr occurred in the entire waterway. The bathymetric analysis of 2011-2013 also indicates a period of accumulation (0.072 m/yr), which can be separated into two parts. First, in 2012, a mean accumulation rate of 0.040 m/yr occurred downstream Verchères, while the sedimentation was null upstream. Secondly, in 2013, a mean accumulation rate of 0.097 m/yr occurred upstream Verchères, while almost no change occurred downstream (accumulation of 0.005 m). The other visible accumulations are usually located near the sides of the waterway or in a migrating dune's field. In addition, punctual recent accumulations were monitored in 2016-2017 in small sectors, but the bathymetric surveys have been intentionally done around accumulation areas and are not representative of the whole waterway.

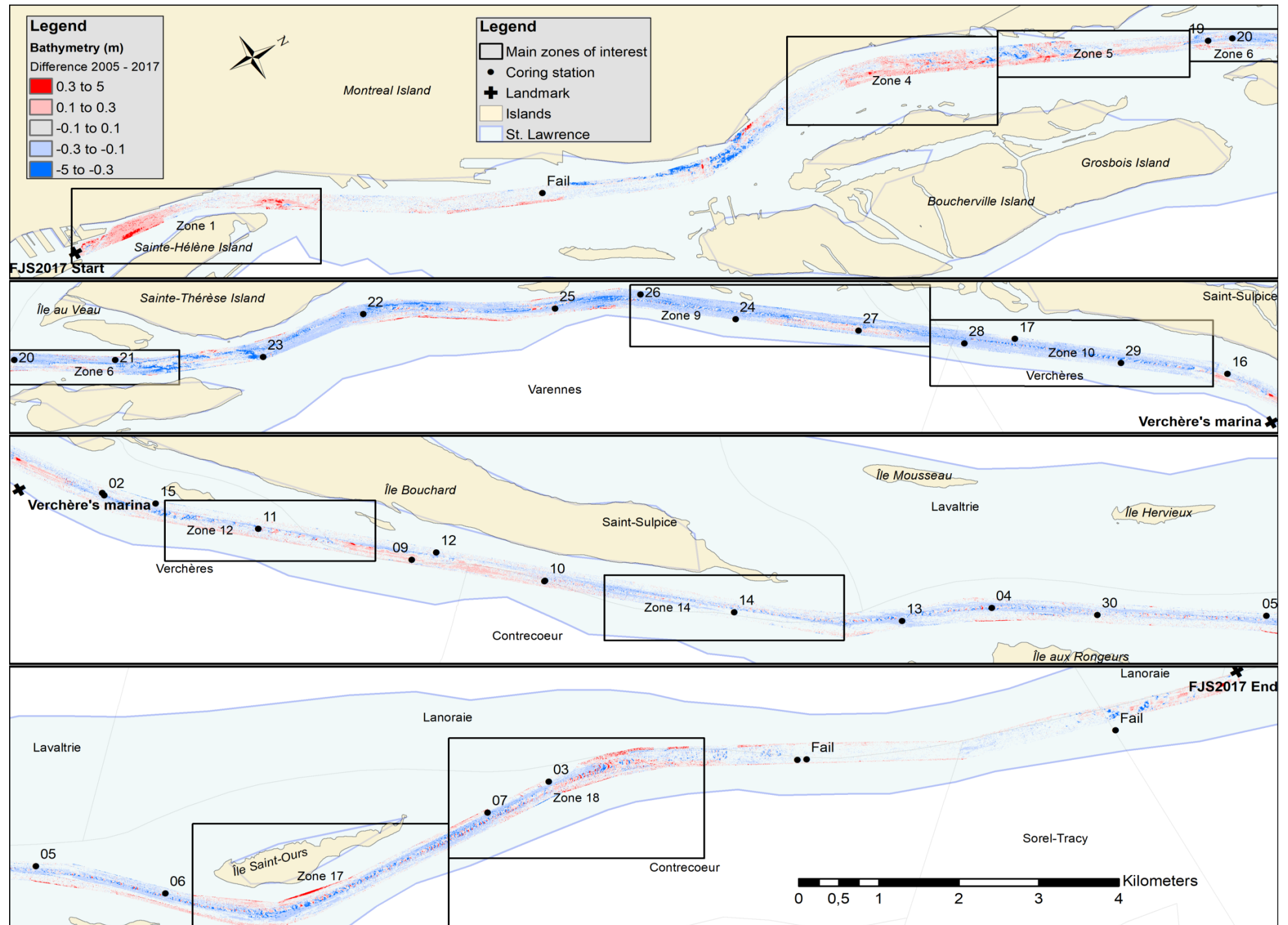


Figure 6. Difference in the bathymetry of the waterway between 2005 and 2017. Red = shallower (accumulation). Blue = deeper (erosion).

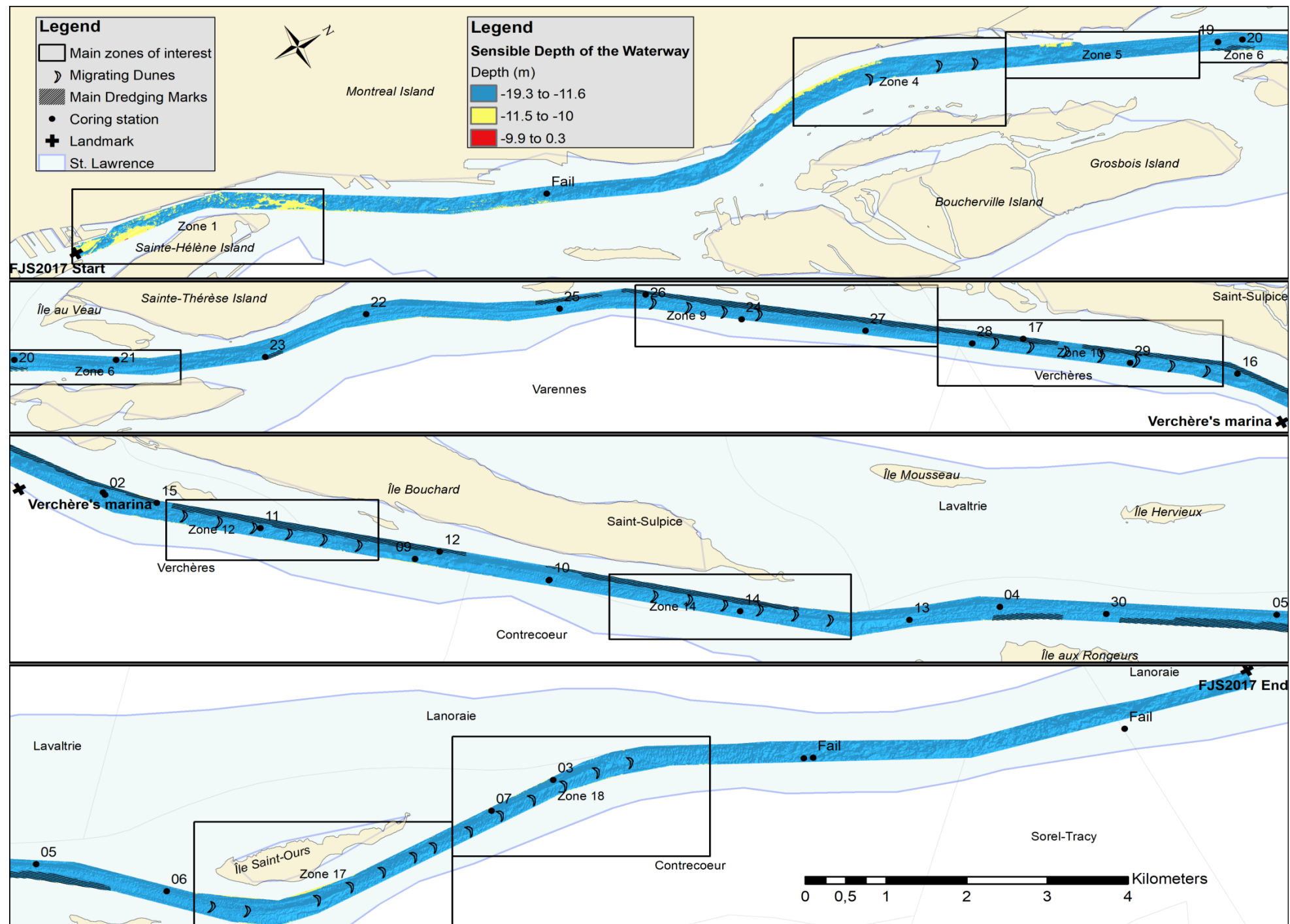


Figure 7. Sensible bathymetry related to the maintained depth for navigation, main dredging marks and fields of migrating dunes.

Dredging marks (Fig 8a and 8b), ribbons and furrows, sandbanks, dunes, surimposed dunes, sand waves, and gravel waves can be identified (Figs 9, 12 and 24) in the waterway according to the classification of large-scale subaqueous bedforms of Ashley (1990). Common dredging marks are differentiated from natural forms by their perfect circular and regular crest spaced at 1-2 m with a height of 0.01-0.05 m (Fig. 8a and 8b). No new marks appeared between 2005 and 2017, plus the visible ones do not migrate (Fig. 8a, 8b, 8e and 8f). The marks are mostly located nearby the waterway sides. The dredging marks could be confused with the small dunes linearly aligned because both are located on the waterway sides, both do not migrate and they have a similar morphology (Fig. 8e and 8g). However, comparatively to the dredging marks, the linearly aligned dunes are 10 times larger. They have a mean height of 0.5 m by 10 m long.

Ribbons and furrows are linear features parallel to the current. They cover most of the riverbed between dunes and dredging marks in the waterway (Figs 8g and 24). Otherwise, the riverbed is plane. The average shape of ribbons and furrows is 2 to 5 m width by 0.05 to 0.2 m height, and their height may change quickly (± 0.6 m/yr).

An uncommon, distinct and elongated form is shown in figure 9. The profile #11 runs through the middle of this form. The base of the form is close to the waterway side, while the head advances in a deeper natural depression in the center of the waterway. Every year, this form is eroded and appears to be a shallow zone on the side of the waterway that was partially dredged.

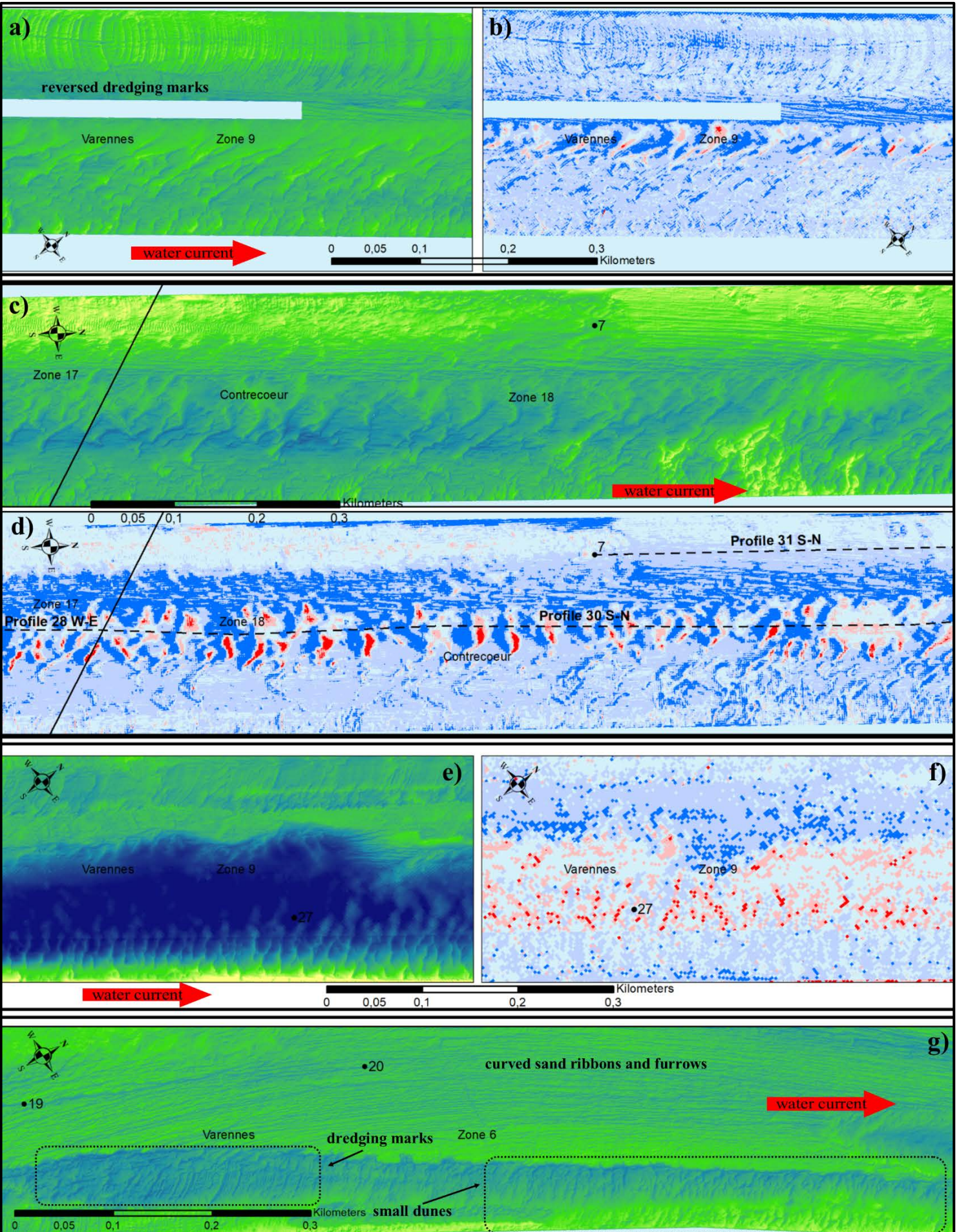


Figure 8. a) Bathymetry and b) depth difference from 2005-2014 which illustrate reversed dredging marks with migrating dunes in the center of the waterway. c) Bathymetry and d) depth difference between 2005-2014 illustrating migrating dunes in the center of the waterway and dredging marks north of the waterway. e) Bathymetry and f) depth difference (between 2005 and 2017) showing disappearing dredging marks, a depression in the center of the waterway, and small dunes linearly aligned close to the bottom edge. g) Bathymetry showing dredging marks followed downstream by small dunes in formation nearby the southern-eastern edge of the waterway, and curved sand ribbons and furrows above.

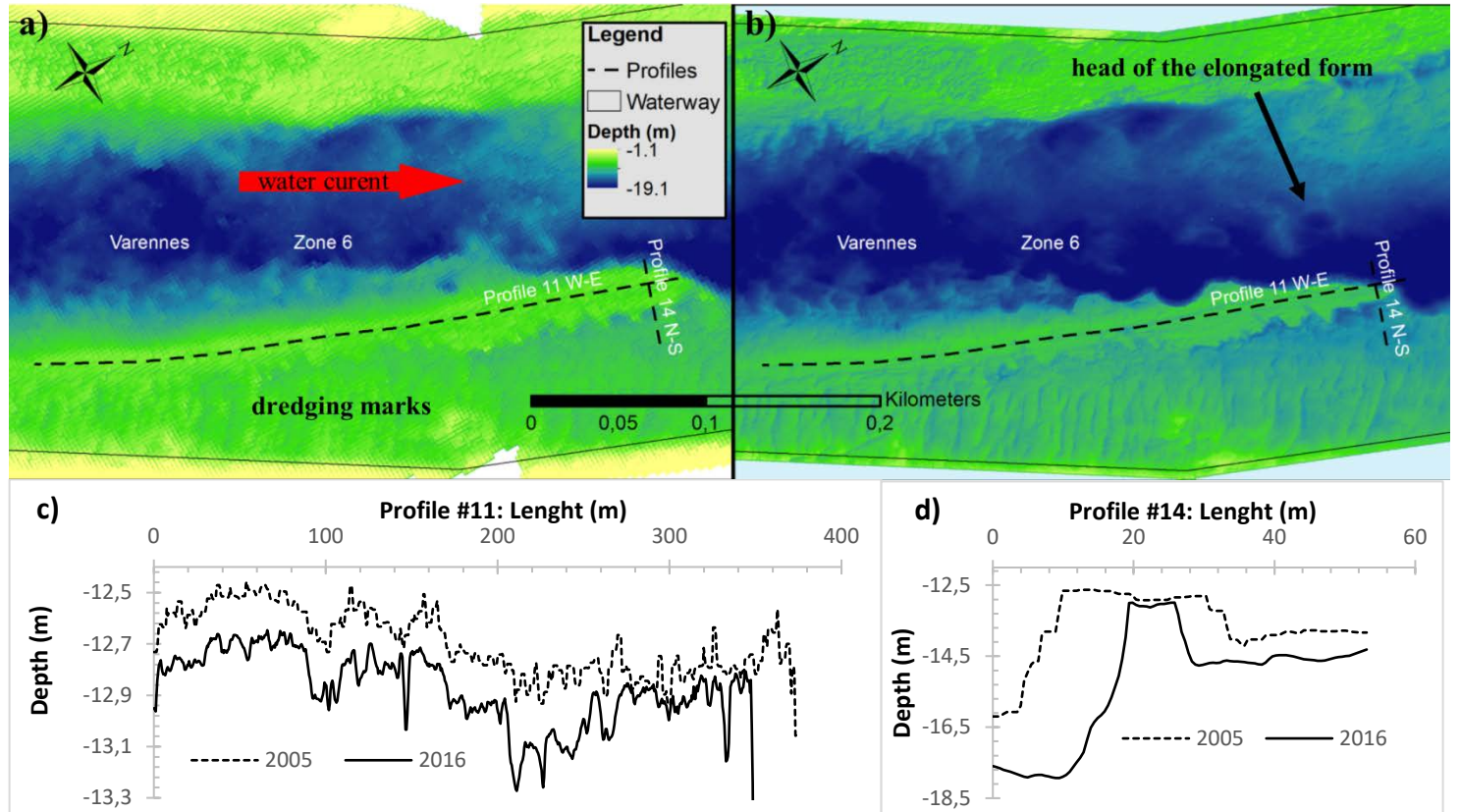


Figure 9. Bathymetry is showing a shallow zone of the waterway partially dredged, then in erosion between a) 2005 and b) 2016. c) Profile 11 shows a mean depth erosion of -0.038 m/yr with a retreat of the head of the form of 24 m upstream. d) Profile # 14 shows a narrowing of the form of 14 m.

As previously mentioned, the smaller dunes on the sides of the waterway do not migrate, while the dunes present in the center of the waterway do migrate (Fig. 7). The migrating dunes are usually sinuous or crescent shaped with the concave side facing the current. The large dunes present a trend for an asymmetrical shape sloping upward, but other dune morphologies are also observable. There are surimposed small dunes or ripples on larger migrating dunes in the waterway (Figs 12 and 24). The migrating dune profile analysis within the zones of interest # 9-10-12-14-17 and 18 demonstrates a mean height of 0.42 m, a mean length of 40 m and a mean downstream migration rate of 1.54 m/yr. On the other hand, two profiles (# 5-6), which are in the zone of interest # 4, show medium

migrating dunes with a mean height of 0.40 m, a mean length of 10 m and a mean downstream migration rate of 3.5 m/yr. Figure 10 is a typical example of dune migration within the waterway that also shows a general erosion of the riverbed.

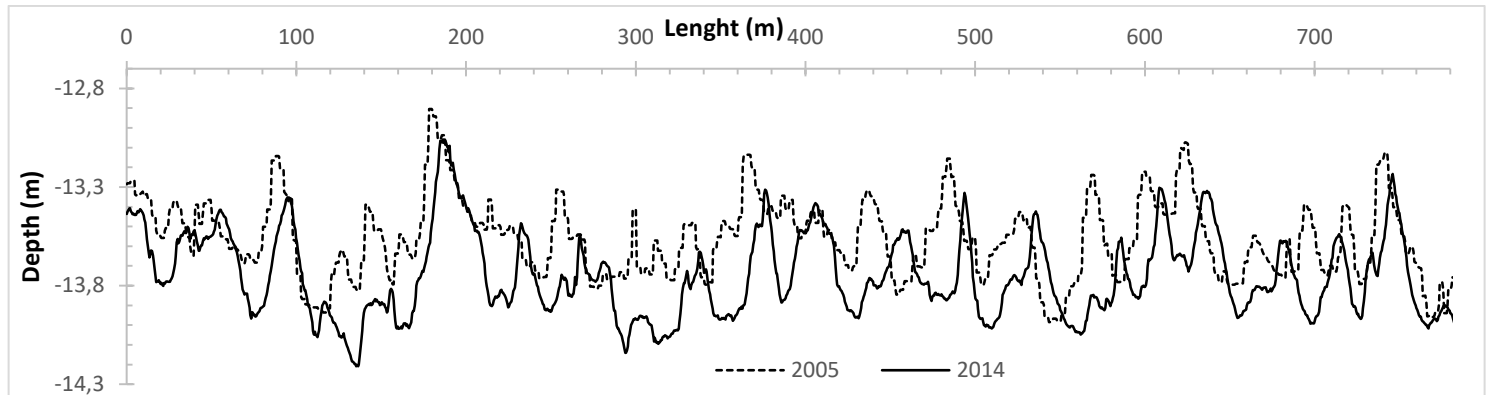


Figure 10. Profile # 30 (plan view represented in figures 6 and 7) showing a field of migrating dunes (1.11 m/yr downstream). The migration is quantified by the migration of the crest between 2005 and 2014.

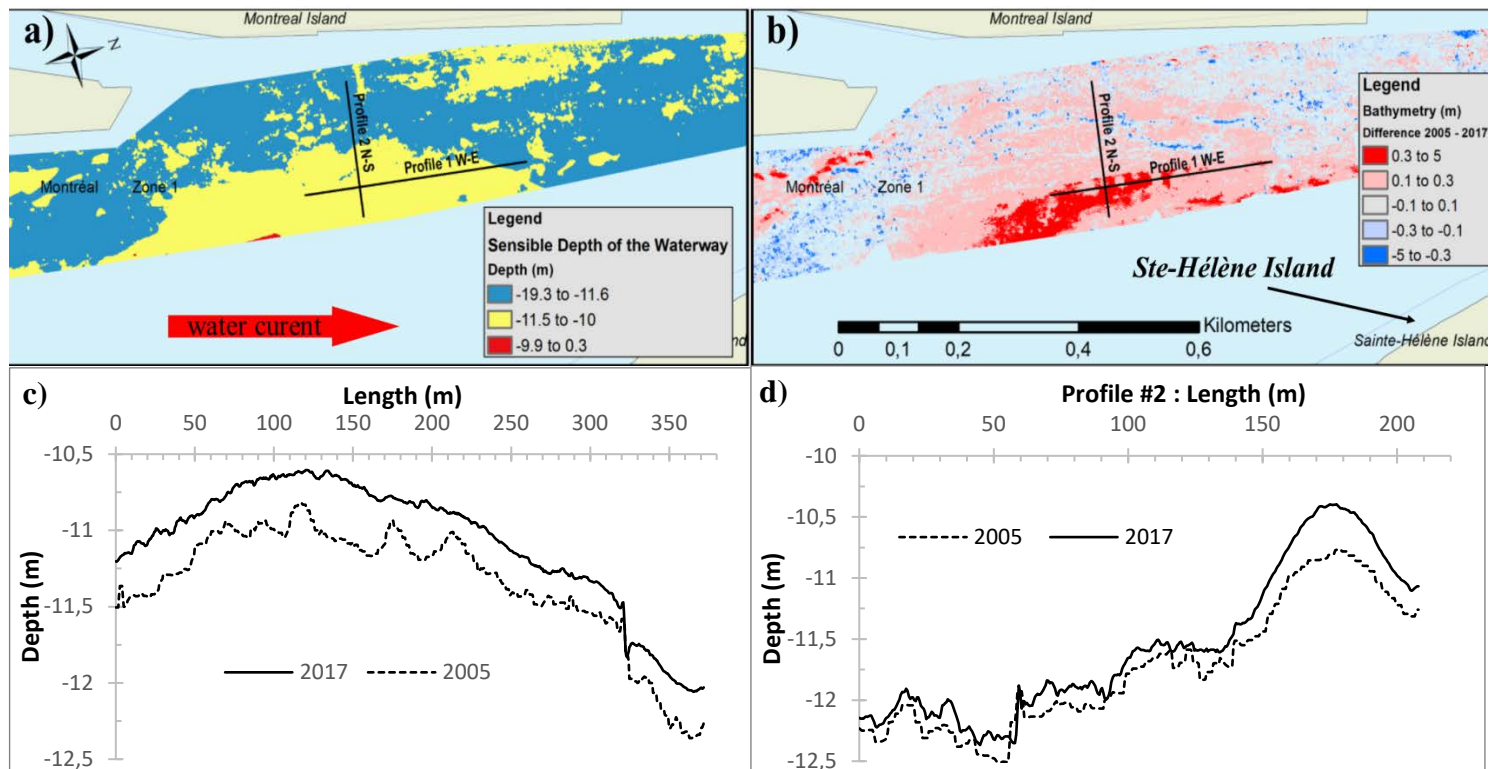


Figure 11. a) Bathymetry of an important accumulation in zone #1 in front of Sainte-Hélène Island and b) difference of bathymetry between 2005-2017 of the same accumulation area. c) South/North profile (#1) indicates a mean accumulation of 0.287 m between 2005-2017 and d) West/East profile (#2) indicates a mean accumulation of 0.184 m for the same period.

Figure 12 presents a sandbank with surimposed small to medium dunes. The forms of this sector change drastically through the years. As a matter of fact, a mean accumulation of 0.019 m/yr has been calculated between 2005-2017, while the smaller surimposed dunes migrated too fast to monitor them via annual survey. The geomorphology of this sandbank is atypical by its circular forms.

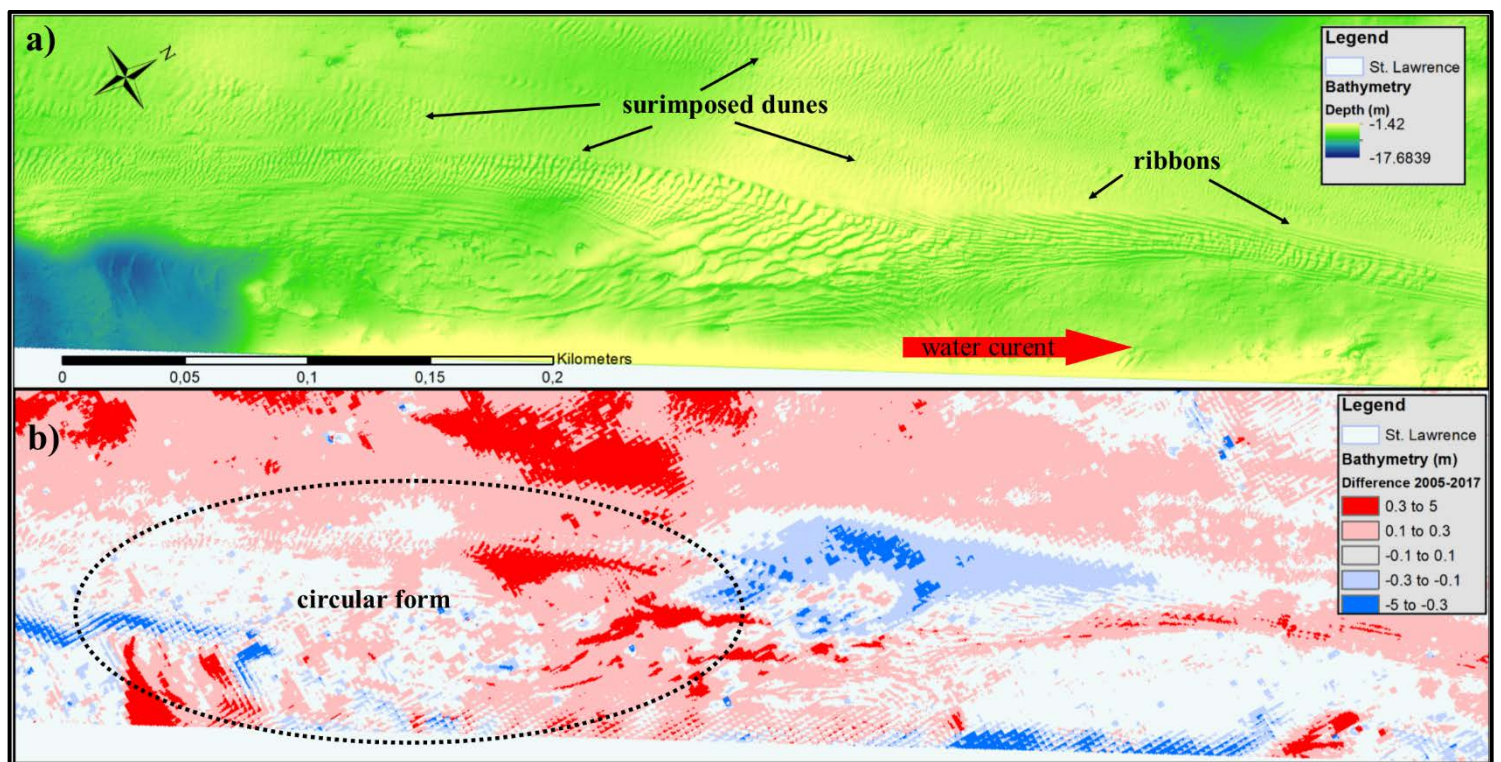


Figure 12. The sector of accumulation at the tip of Sainte-Hélène's Island. Dunes of different geometries, ribbons and circular forms are creating a sandbank, visible with a) bathymetry and b) the difference in bathymetry between 2005 and 2017.

1.5.2 Surface sediments

Grain size

The grain size distributions of the surface sediments demonstrate the dominance of fine sediments (clay and silt) along the waterway. This dominance is also notable in the gravity core # 03. Indeed, most of the samples (16 samples on 23) are characterised as «mud» or «medium silt» with less than 10% of sand. Coarse sediment samples are classified as sandy mud (# 21-17) and gravelly mud (# 23, 11). They are located near the sides of the waterway. The surface samples # 08, 22 and 04 are likewise dominated by gravel mixed with sand and clay. Samples # 04, 11, 08 and 10 have been sampled on dune fields, while other coarse sediment samples were sampled in erosive areas with strong bottom currents (Fig. 6). Figure 13 shows that all samples contain more than 5% of clay, even those dominated by coarse sediments. The surface sediments are poorly sorted and most of them have a polymodal distribution. If the coarse sediments mentioned above are ignored, the D₅₀ (median) of the combined distribution of all samples is $3 \pm 1 \mu\text{m}$ and the D₉₀ is $13 \pm 4 \mu\text{m}$. Those values indicate the importance of very fine clay in the surface sediments.

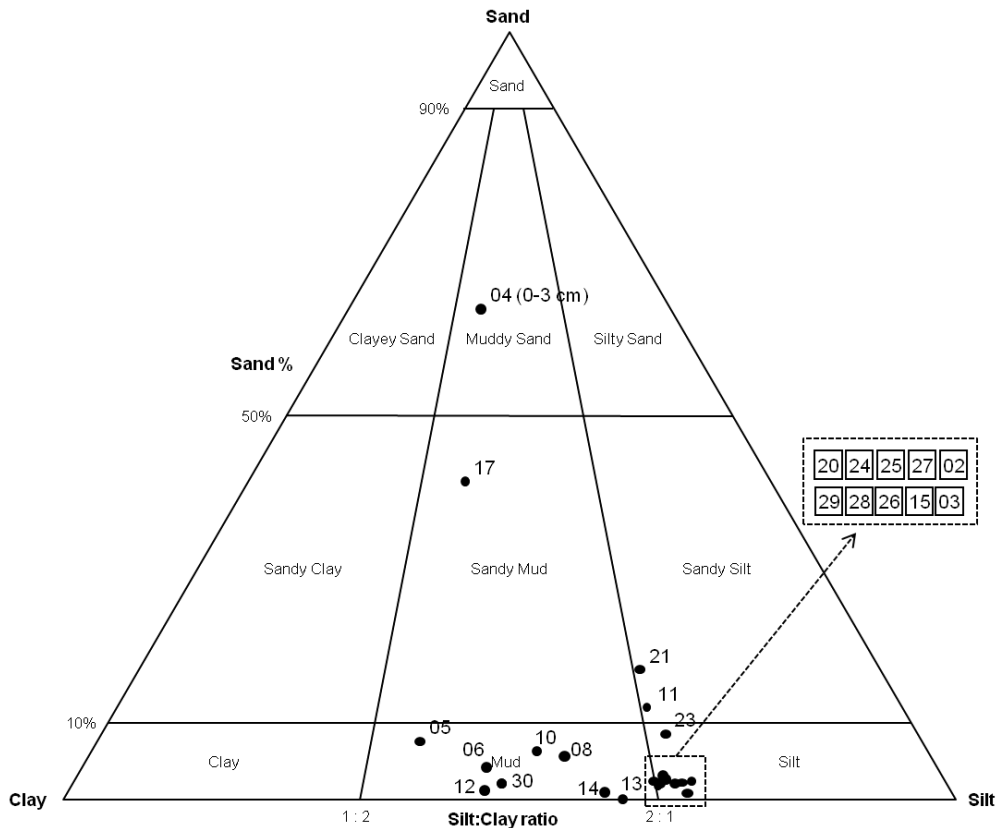


Figure 13. Clay-silt-sand ternary diagram representing the surface samples (0-1 cm) of every core from FJS2017 mission. The core number is indicated for each sample. Core #22 is out of range because it contains a significant amount of gravel. (Modified from GRADISTAT 2001 software.)

Carbon and water contents

The total carbon (TC) content of the surface sediments measured on every short core varies from 0.5 % to 2.3 %. Most of these measures are inferior to 1.6 % (Fig. 14), except for the cores # 17-30-06 that have higher TC due to their inorganic carbon (IC) content. Figure 14 demonstrates the remarkable constancy of the organic carbon (OC) along the riverbed of the waterway, in opposite to the TC and IC. The mean carbon contents and their respective confidence intervals (1σ) demonstrate the same observation: $OC = 0.43 \pm 0.07 \%$, $TC = 1.04 \pm 0.43 \%$ and $IC = 0.61 \pm 0.42 \%$. Furthermore, the mean water content of all the

surface samples is $36.0 \pm 5.9\%$ and the drier surface sediments (less than 30%) are from the cores # 11 (24.7%), # 12 (21.7%) and # 04 (21.3%). Core # 04-11 contain coarser sediments and core # 12 was sampled on dredging marks.

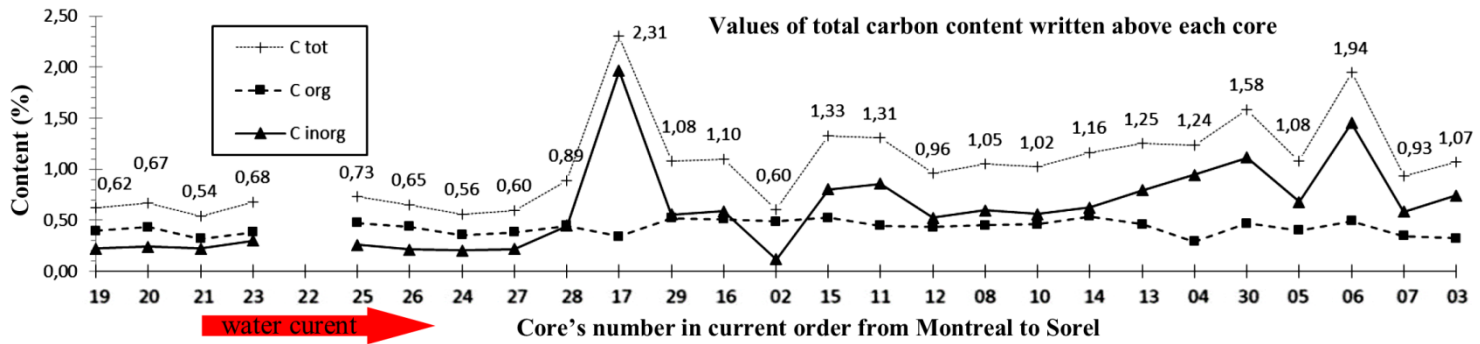


Figure 14. Carbon contents in surface samples from Montreal to Sorel: total carbon (TC), organic carbon (OC) and inorganic carbon (IC). The space between cores is not representative of the distances. Core # 22 is mainly composed of gravel and sand. No carbon analysis was completed for this core

1.5.3 Short sediment core

Visual description

The visual description of the cores highlights the dominance of the fine sediments with depth, even for those constituted of coarse sediments at the surface. Most of the cores, except cores #22-04-11 and 17, show traces of bioturbation in the first 5 cm. Core #22, which was sampled in an erosive area, is composed of gravel mixed with sand and clay in the first 9 cm, but the granulometry becomes finer with depth. The three other unbioturbated cores are also composed of coarse sediments at the surface, but become dominated by fine sediments after 7 cm for cores # 04 and 3 cm for cores # 11-17.

The fine sediments are dark grey with olive green and brown color variations (Fig. 15). Core #16 is the only one that shows an abrupt change in color which becomes red

below 18 cm. The other parameters of this core (density, "P" wave velocity, carbon contents and chemical composition) do not show important changes. Half of the short sedimentary cores are finely laminated and organic-poor (Fig. 15c). The laminations are constituted of changes in grain size, color, and wet bulk density. Individual laminae are usually 0.5 cm thick or thinner with some laminae around 1 cm in thickness. At the opposite, the other half of the cores are not laminated and contains numerous black scattered pieces of organic matter the size of spruce needles or smaller into a homogeneous fine matrix of grey clay (Fig. 15a). The laminated cores are located downstream of the marina of Verchères (more precisely downstream core #15), while the unlaminated cores are mostly upstream the marina (Fig. 3).

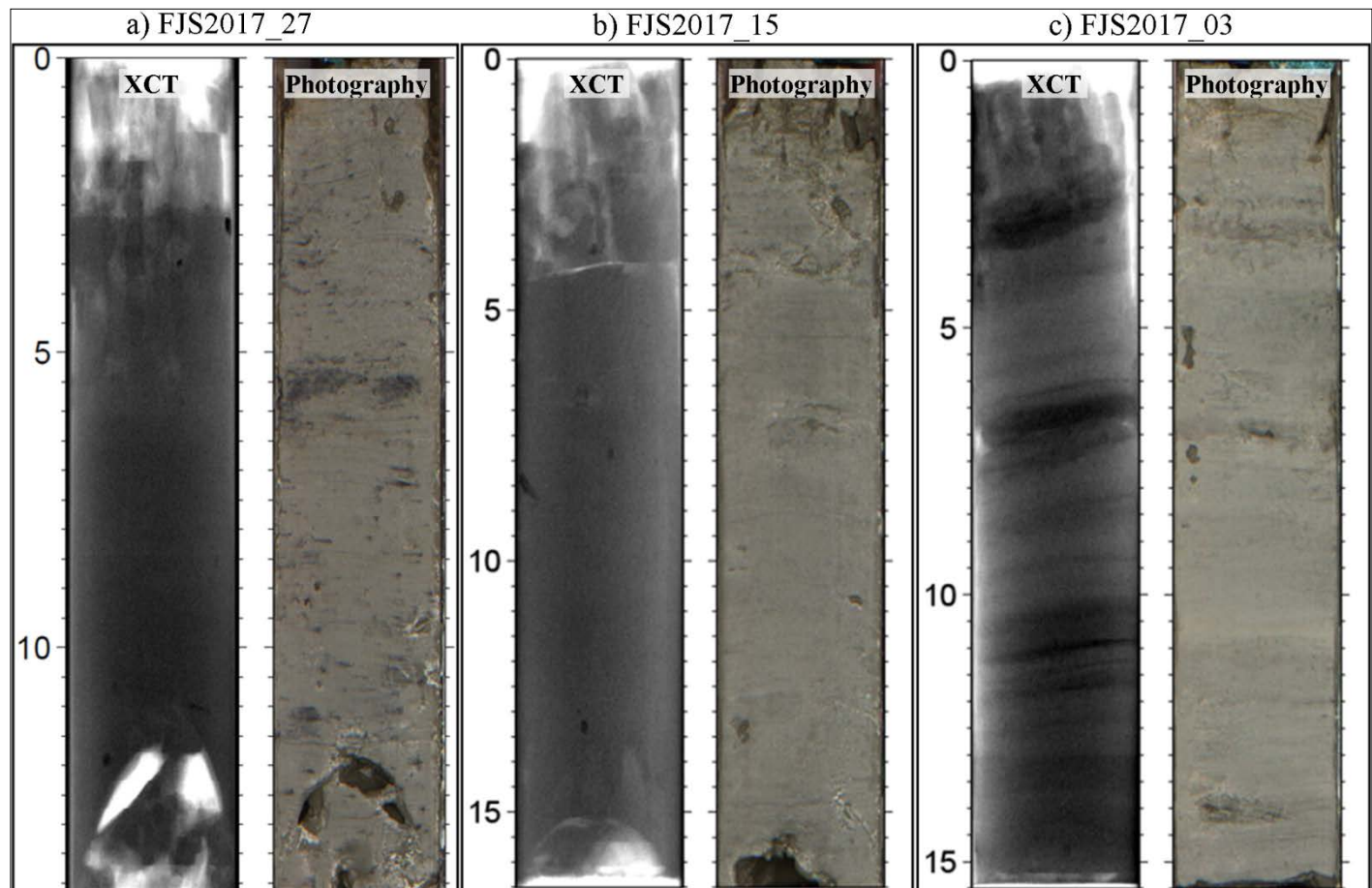


Figure 15. X-ray image and photography of a) unlaminated core with evident OM (FJS2017_27); b) unlaminated core with less OM (FJS2017_15); c) laminated core (FJS2017_03).

Grain size and carbon content of short cores

The grain size analysis of core FJS2017_03 illustrates a narrow grain distribution between “clayey silt” or “silt and clay” (Fig. 16). The carbon analysis along the three cores # 03, 16 and 19 indicates similar results between them. The mean TC contents of the three cores are effectively comprised between 0.54 and 1.59 %. Moreover, the OC content is low and remarkably constant. It varies between 0.20% and 0.51% (Fig. 17). Core # 03 is one of the most clearly laminated cores and these laminations affect the total carbon curve compared to the core # 19. This core is unlaminated and contains around 0.51% less TC content than cores # 03 and 16.

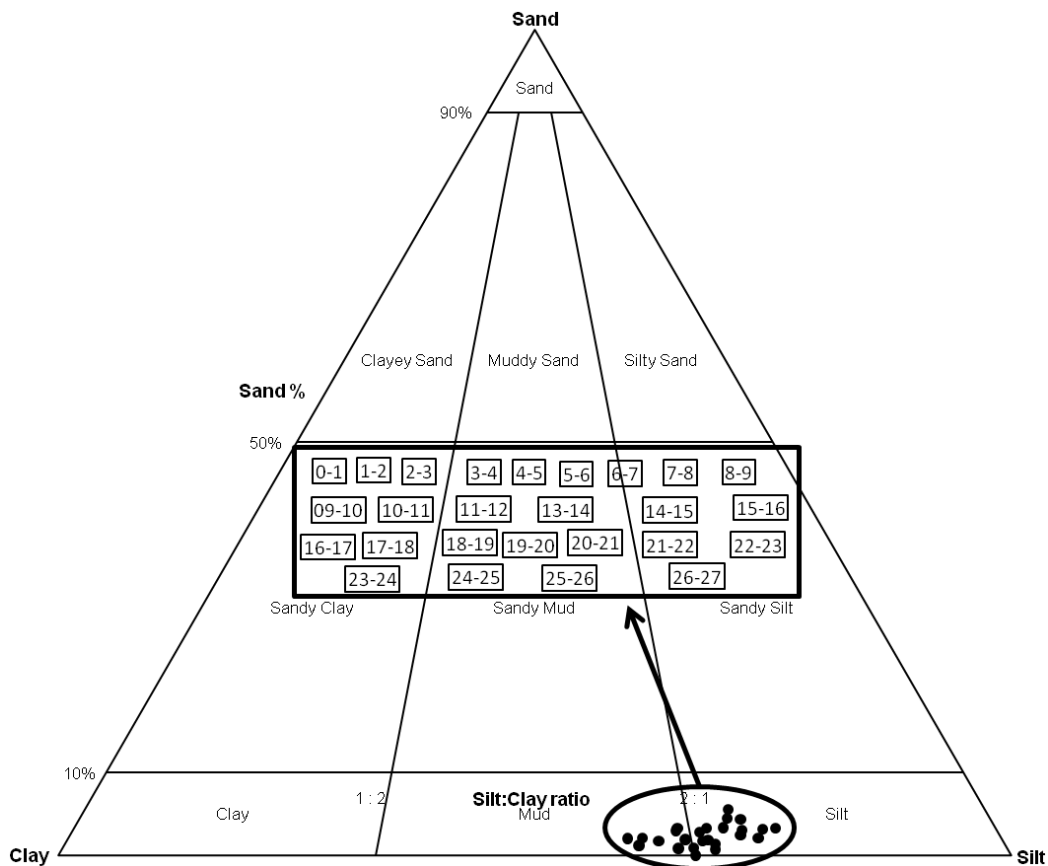


Figure 16. Clay-silt-sand ternary diagrams of the core FJS2017_03. The box indicates the depth of each sample analysed. The diagram shows the dominance of fine sediments and the relative uniformity of the grain size along the core. (Modified from GRADISTAT 2001 software.)

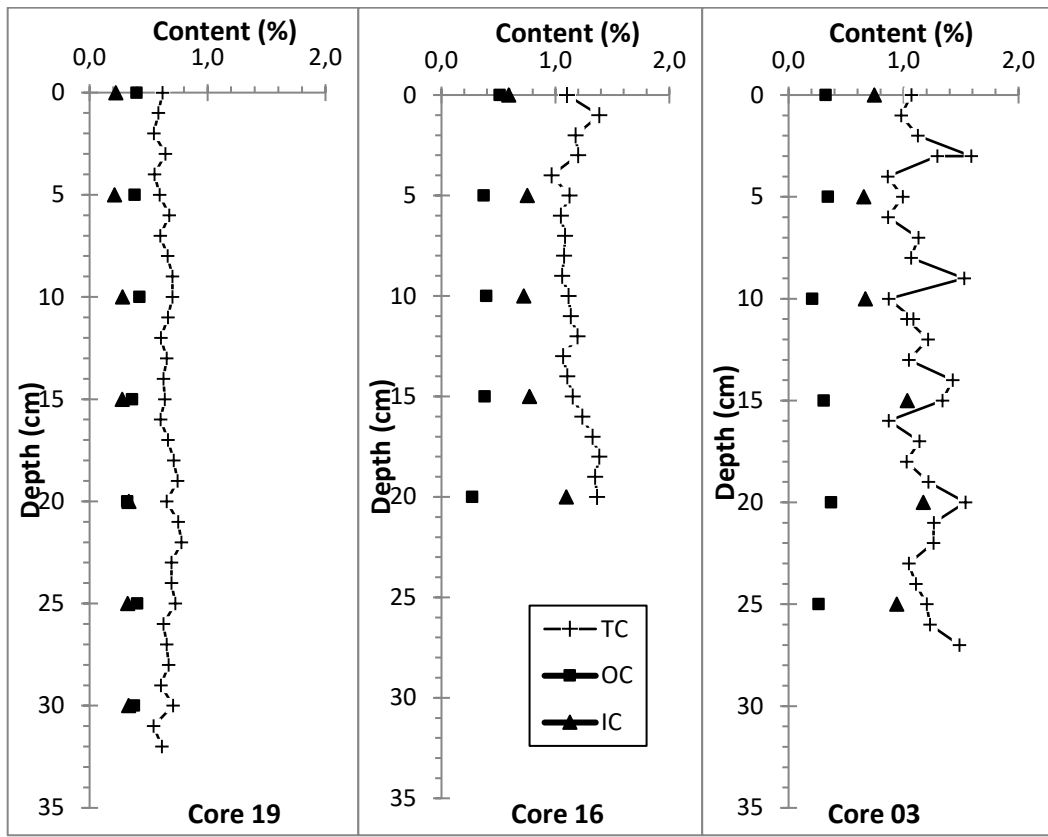


Figure 17. Carbon contents of the cores # 19, 16 and 03: total carbon (TC), organic carbon (OC), and inorganic carbon (IC) contents. Core # 19 contains less carbon than the two others and its values of carbon contents are more constant.

"P" wave velocity, wet bulk density and water content

Like visual descriptions, the quantitative analyses performed in the laboratory with the MSCL on each core indicate similar characteristics between the cores. The overall mean p wave velocity is 1619 ± 34 m/s and the mean density is 1.33 ± 0.08 g/cc (Fig. 18). This last figure also illustrates the positive relation between the velocity and the bulk density. Figure 19 illustrates that the mean water contents of the cores are relatively constant: core # 19 (41.7 ± 3.7 %), core # 16 (41.8 ± 0.8 %), core # 07 (35.6 ± 2.7 %) and core # 03 (31.4 ± 2.9 %). On the other hand, cores # 07 and 03 show downcore variations of the water content unlike cores # 19 and 16. In addition, cores # 07 and 03 are denser (Figs 18 and 15) and present distinct laminations.

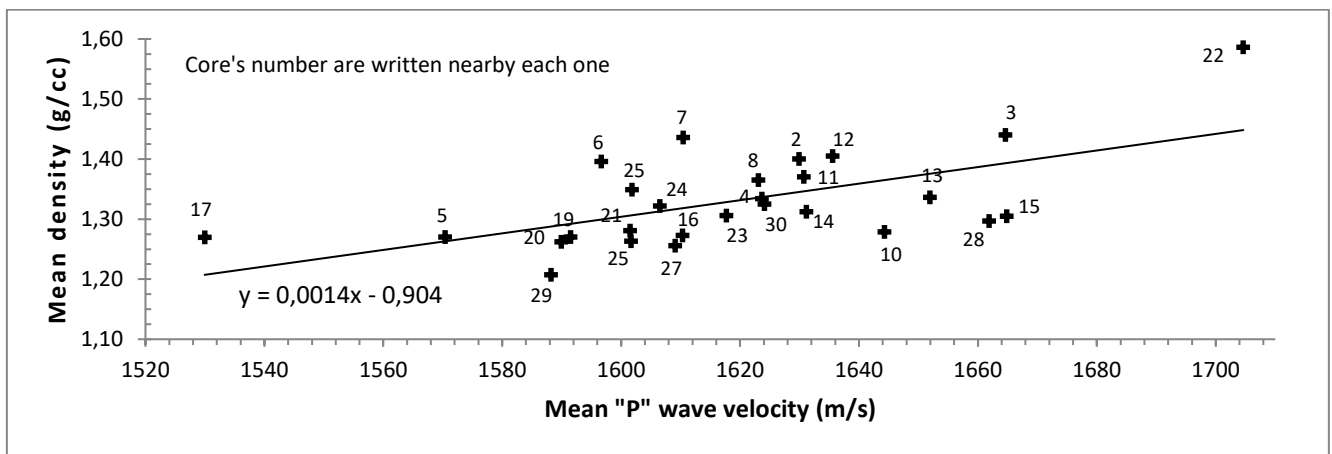


Figure 18. Wet bulk density versus "P" wave velocity for each core. A positive correlation is visible between the two parameters. Core #22 is mainly composed of coarse sediments (gravel).

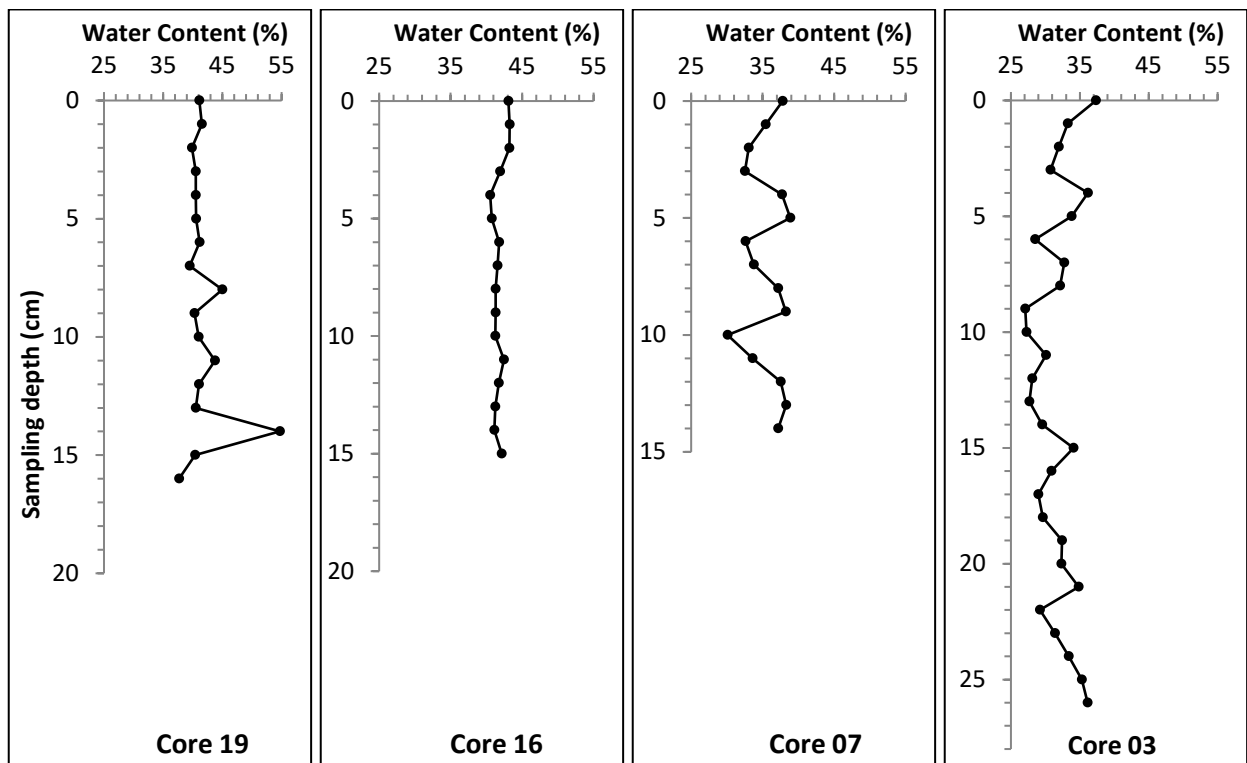


Figure 19. Water content in cores # 19-16-07-03. The water content in the cores # 07-03 show downcore variations unlike cores # 19-16.

1.5.4 Chronology

The results of ^{210}Pb activity determined on the three cores # 19-16-07 show no radioactive decay (Fig. 20) and the values obtained are relatively constant. In consequence, no sedimentation rate could be calculated. In addition, the ^{210}Pb activity is similar to the values reported for the supported ^{210}Pb in cores from the St. Lawrence River system (e.g. Cauchon-Voyer et al., 2008; Zhang, 2000) suggesting the presence of relatively old sediments at the surface. This is confirmed by the age of 11 640 cal BP determined on a pelecypod shell sampled at 7-8 cm in core FJS2017_16. This age is coherent with the work of Occhietti and Richard (2003) which dated the regional marine invasion of the Champlain Sea in St. Lawrence Lowlands from 13.15 to 10.6 cal BP.

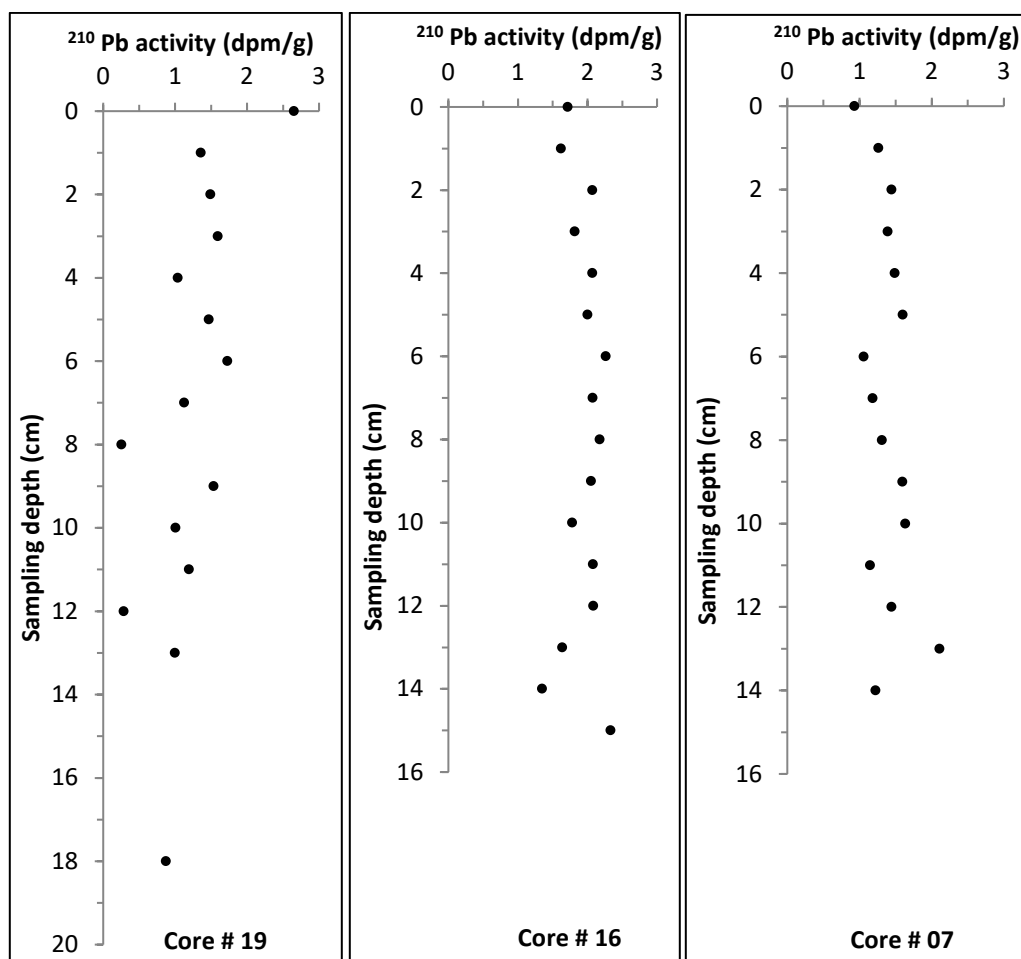


Figure 20. ^{210}Pb activity for cores # 19-16-07.

1.5.5 Seismo-stratigraphic Units

Previous high-resolution seismic surveys accomplished in the Estuary and Gulf of St. Lawrence (Heiner and Scott, 1999; St-Onge et al., 2008; Syvitski and Praeg, 1989) provide the seismo-stratigraphic framework. In chronological order, are presented: 1) ice-contact sediments (till); 2) glaciomarine sediments including ice-proximal and ice-distal sediments deposited during the marine invasion and its retreat; 3) postglacial sediments. The present seismic survey covers a fluvial portion of the St. Lawrence and reveals a similar stratigraphic sequence (Figs 21-22). The 148 linear km of seismic data are separated in 13 continuous lines located approximately in the center of the waterway and paralleled to it. In addition, 157 lines that cross over the channel were acquired (Fig. 3).

Unit 1

Unit 1 represents the acoustic basement and is characterised by the absence of acoustic penetration and a relatively smooth morphology. The upper boundary of this unit is defined as a single high amplitude reflection where it outcrops (Fig. 21, line 0004_298 in line with the borehole B_2165). Past dredging works affect this unit upstream Longueuil and consequently create a straight and rugged surface. Veneers of sediment frequently overlie the acoustic basement where the latter reaches the surface. Those veneers thus create a thin (< 0.01ms) double reflection only where unit 1 outcrops. Ripple forms of 0.5 m to 2 m high by 5 m to 100 m long are clearly and frequently visible where a veneer is present (see U1 in Fig. 21).

Unit 1 is the oldest unit and it outcrops from Montreal to Ste-Thérèse Island on the entire waterway. This unit then plunges and disappears until it shortly reaches the subsurface in front of Verchères. Unit 1 dips downstream (Fig. 21, Line 0001_297), and the signal of Unit 1 is lost below the thick sedimentary sequence above, around 1 km after the "Île-aux-Prunes". This unit is not visible when the seismic acquisition is realised outside of the waterway or where a high to very high amplitude reflector overlies it.

Unit 2

Unit 2 is semi-transparent with low to medium attenuation of the acoustic signal. It usually presents an irregular and sometimes chaotic surface. This unit does not drape the underlying one and often presents a sinuous upper boundary with punctual (sometimes numerous) high amplitude reflections. Unit 2 sometimes appears as the acoustic basement because of its high amplitude reflections, which also limits the acoustic penetration. However, unit 1 intersects unit 2 where a sudden rise of each acoustic unit is visible (ex: in front of Verchères and Ste-Thérèse Island). The upper boundary of unit 2 is sometimes closely draped by a thin (< 1.5 m) reflector of high amplitude. The boundary is in consequence less defined and more chaotic. The *ArcGIS* borehole database indicates the presence of sand and gravel layers within this unit. Those layers could interfere with the delimitation of the upper and lower boundary and could contribute to the chaotic aspect of this layer.

Unit 2 appears first in front of Ste-Thérèse Island and maintains a general depth (from water level) between 19 m and 24 m. Unit 2 reaches its maximum depth of 37 m in front of the terminal of Contrecoeur and disappears downstream under the sedimentary cover. The thickness of this layer is not assessable due to the limitation of the acoustic penetration.

Unit 3

Unit 3 is the most widespread unit and it consists of low to high amplitude parallel reflections (Fig. 22, line 0003_297). This unit is also characterised by noticeable transparency between parallel reflections and a progressive attenuation of the acoustic signal. Usually, the parallel reflections are well-defined and continuous. They also conformably drape the underlying unit. The upper boundary of this unit is the interface water/sediment. This boundary mostly presents a well-defined and thin (< 2 m) double reflection (Fig. 22, upper panel). The upper reflection is of high amplitude while the contiguous underlying reflection is low amplitude. The sinuous upper boundary often forms

ripples with the same sizes as unit 1, except where the interface is erratic and does not allow a good definition of the boundary. The double reflection is probably due to the presence of a veneer of coarse sediments over the unit 3, because it is present where the bathymetry show ripples on the riverbed. The depth of this unit reaches 36 m in downstream the terminal of Contrecoeur (Fig. 22, Line 0003_297) and the thickness varies from 0 to 23.2 m along the waterway. The depth range of the acoustic penetration is limited by the presence of coarse and dense sediments, often spread or layered in Unit 2. The short sedimentary cores recovered in this study represent the water/sediment interface of Unit 3.

Two subunits are distinguishable in unit 3 as shown in figure 22. Subunit 3a seems to outcrop upstream of the "Île-aux-Prunes", while subunit 3b outcrops downstream. Subunit 3a consists of two parallel reflections of medium to high amplitude separated by a transparent lens of varying thickness. The upper boundary is a wavy surface. Under those two reflections, a fine laminated to transparent facies follows. It presents a varying thickness according to the depth of the underlying unit 2. This subunit is disturbed upstream the marina of Verchères and thus presents a chaotic facies (Fig. 21, line 001_298). The *ArcGIS* boreholes B_2363 and B_2364 near the seismic line 0002_298 (respectively at 67 m and 26 m of distance) describe this subunit 3a as compact sand and clay. Subunit 3b consists of a series of parallel and continuous reflections of low to medium amplitude with a progressive attenuation of the acoustic signal. Downstream core FJS2017_30 (Fig. 22), several high amplitude and almost tabular reflections limit the penetration of the acoustic signal below the water/sediment interface. The subunit 3b reaches a 35 m depth near the end of the studied area; around 200 m upstream core FJS2017_07.

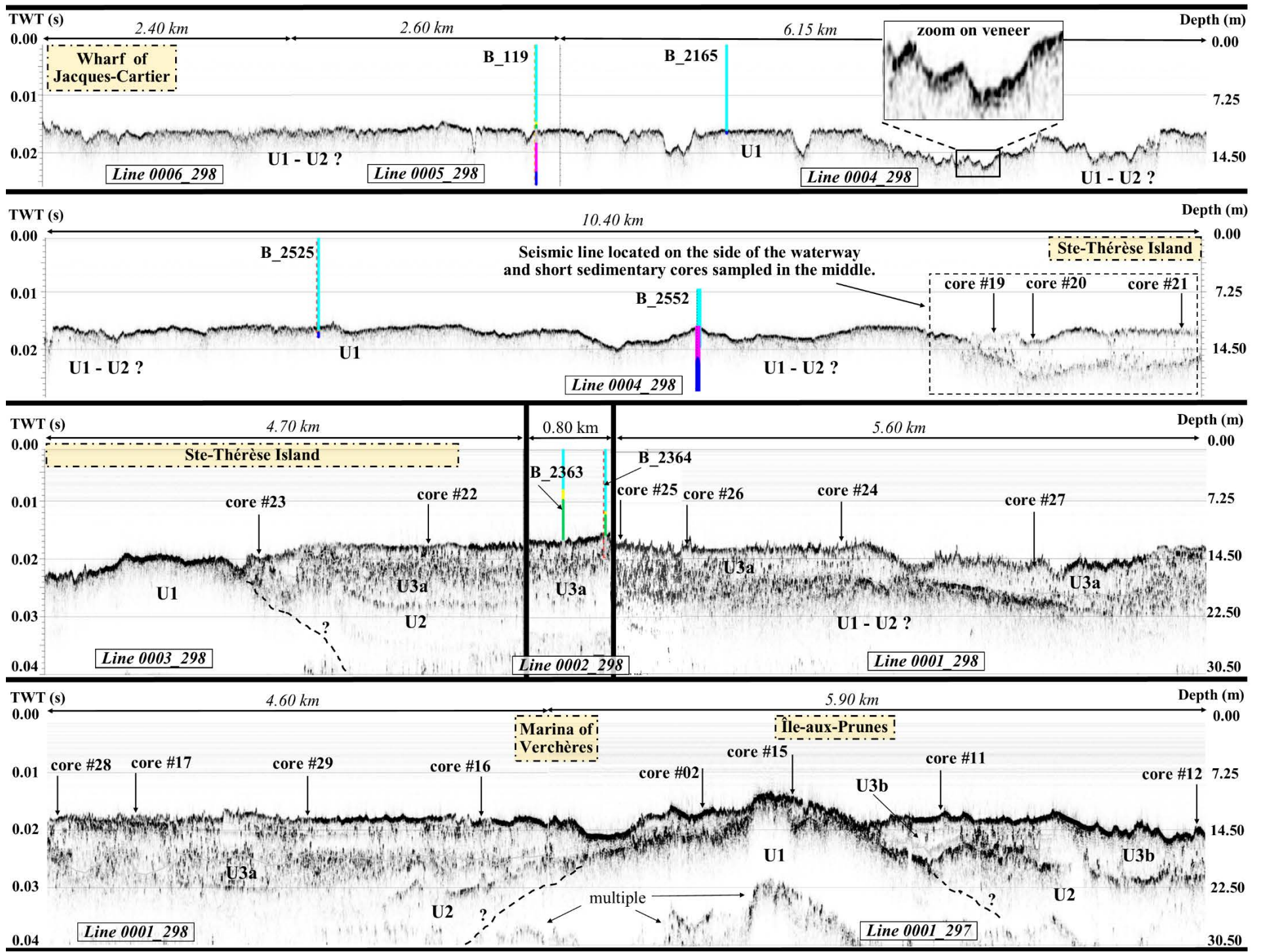


Figure 21. Quasi-continuous seismic lines from the Jacques-Cartier wharf (Montreal) to the marina of Verchères (lines 0006_298 to 0001_297).

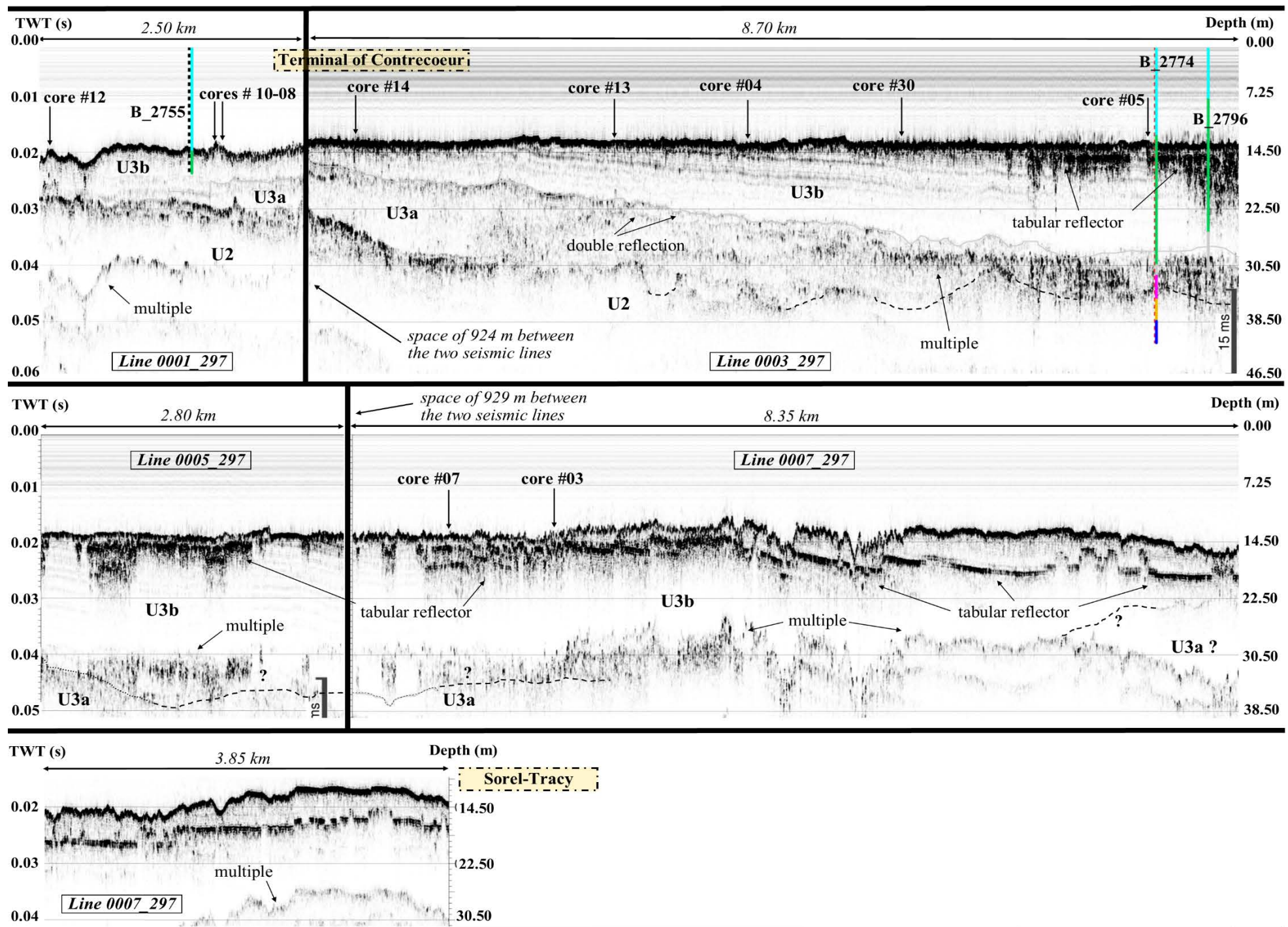


Figure 22. (Following figure 21) Quasi-continuous seismic lines from the marina of Verchères to end of the studied area (lines 0001_297 to 0007_297).

1.6 DISCUSSION

1.6.1 Chronostratigraphy

The seismic lines reveal two main changes in the stratigraphy that affect the sedimentary processes. The different types of cores observed in the waterway are therefore related to those changes. The veneers of coarse sediments sometimes visible on seismic profiles are located on dune fields and thus correspond to recent sedimentation in the waterway. On the other hand, the majority of the cores sampled during the FJS2017 mission represent fine grained sediments because the sections of the riverbed with coarser sediment are mostly too dense to allow the penetration of the gravity corer used.

Unit 1 is interpreted as the bedrock (probably the Shale of Utica as described by Chen et al. (2014); Lavoie et al. (2014); Séjourné, S et al. (2013); Thériault (2012)) or ice-contact sediments. Previous dredging works of the Port of Montreal and *ArcGIS* boreholes (ex: B_119, B_2165, B_2525) also described the presence of the black shale near the surface. The recurrent accumulation in the zones # 1 to 5 (Figs 3, 6 and 7) is spatially related to the outcrop of the bedrock. The hydrodynamic regime of this sector is probably the main cause of the sedimentary accumulations observed. Rondeau et al. (2000) reported that 70% of the water flow in the St. Lawrence River passes within the navigation channel, and the current velocity varies between 0.7 to 3 m/s. Some hypotheses can explain why there is more accumulation close to Montreal. 1) The difference of the flow inside the channel compared to the rest of the river just beside is probably a lot different where the black shale outcrops than where the clays outcrop, because the navigation channel needed more excavation close to Montreal than downstream Ste-Thérèse Island. The variations of the bathymetry (inside versus outside the channel) influence the current velocity and thus the sedimentation. Carignan and Lorrain (2000) even described net sediment accumulation of 1 to 18 kg/m²/yr outside the main channel, where no accumulation occurs inside. 2) Turbulence is probably greater upstream Ste-Hélène Island due to: the presence of infrastructures (the Beauharnois hydroelectric dam, Champlain's Estacade located upstream the bridge and the pillars of the bridge), the outcrop of the till and the bedrock that involve a rougher riverbed than the clay

downstream Montreal, and the Lachine Rapids. The greater turbulence increases sediment suspension, while the zones #1 to 5 are relatively calmer and allow the deposition of coarse sediments. 3) Since 1959, the use of the St. Lambert lock promotes erosion and adds suspended sediments in the river close to this area.

However, measurements of the currents with instruments such as Acoustic Doppler Current Profilers (ADCP) should be carried out in the navigation channel to validate those hypotheses and create local current models. Hence, this part of the waterway is the only one where the water depth is problematic regarding the objectives of the Port of Montreal (11.3 m maintained) and a close monitoring is suggested. The plunge of Unit 1 in front of Ste-Thérèse Island (Figs 3 and 21, line 0003_298) marks the apparition of the other units and an important change in the sedimentary processes. This plunge corresponds to a normal fault of the bedrock known as "Bas-de-Sainte-Rose" Fault (Gélard et al., 1992; Séjourné, Stephan et al., 2002). From that point, the general trend of erosion begins and the large dunes appear in the waterway.

Unit 2 is interpreted as ice-contact sediments (till) and may be overridden by major glacial advances reported by Lamothe (1985). This unit could even be the result of several glacial invasions and ice retreat episodes between the Illinoian and the Late Wisconsinan according to Lamothe (1985); Occhietti (1990); Parent and Occhietti (1988); Prest et al. (1982). Prest et al. (1982) suggested that "two episodes of Wisconsinan Glaciation referred to as Malone and Fort Covington were responsible for the deposition of two till sheets" on the Island of Montreal and its surroundings. The presence of those two tills is also mentioned in Rosset and Chouinard (2009) and the borehole descriptions from a report of Golder Associés Ltée (2009) (including B_119 in figure 21) described different layers of till. They described the till as compact to very dense, usually composed of various amounts of gravel, sand, silt, clay and pebbles, and presenting a dark grey or dark brown color. The seismic resolution of the present study does not allow a differentiation of such particularities within Unit 2, which could be useful to determinate the extent of those two tills.

Unit 3 is interpreted as glaciomarine sediments and many previous studies have also described similar characteristics in glaciomarine sediments from the St. Lawrence Estuary (Duchesne et al., 2007; Normandeau et al., 2015; Parent and Occhietti, 1988; St-Onge et al., 2008). The glaciomarine package firstly outcrops with subunit 3a and it corresponds to the two types of unlaminated short sedimentary cores (Figs 3 and 15). Subunit 3a outcrops from "Bas-de-Sainte-Rose Fault" up to the stratigraphic threshold in front of "Île-aux-Prunes" (core #15), plunges and underlies subunit 3b. Subunit 3b secondly constitutes the riverbed downstream the threshold. Its sharp contact with the underlying subunit 3a indicates a rapid change in glacial sedimentary supply. The *ArcGIS* boreholes B_2774 and B_2796 also confirm the continuity and the stratigraphic sequence of both subunits (Fig. 22). The stratigraphic threshold produced by the rise of the bedrock (or till) intersects every unit above. It marks another significant change in the characteristics of the short cores and the recent sedimentation (last 13 years), as explained for the year 2012 in the bathymetric results (p. 22-23). This rise of the bedrock is corroborated by the work of Thériault (2012) which created a map of the residual component of the total magnetic field and a map of the Bouguer anomaly showing the prolongation of a positive anomaly passing through the threshold at "Île-aux-Prunes". Séjourné, S et al. (2013) also indicated the presence of important normal faults which can explain the sudden uplift of the stratigraphic unit and their rapid plunge just after (Fig. 22, line 0001_297 and 0003_297).

The subunits 3a and 3b compose the Champlain Sea Clays and are contrasted by the laminated/unlaminated aspect observable both on seismic data and core analyses. Similar seismic characteristics as the subunits 3a and 3b are described by Normandeau et al. (2013, 2017) in the stratigraphy sequence of Champlain Sea deposits at Lake St-Joseph (Québec). The Champlain Sea Clays are described by previous studies as "silts, silty clay and clayey silt sometimes laminated and locally including rhythmites" (Catana, 2006; Dion, 1977; Gadd, 1971; Lamothe and St-Jacques, 2015; LaSalle, 1963; LaSalle and Elson, 1962; Russell and Cummings, 2009; Woodley, 1996). The grain size distribution of every sample is dominated by clays and is coherent with previously described Champlain Sea Clays. In addition, the ^{14}C age (11 640 yr cal BP) determined from the marine shell and the

continuity of the seismic units indicate that the sediments of the core # 16 (subunit 3a) and the other cores upstream date from the Champlain Sea episode (Duhaime et al., 2013; Gadd, 1971; Occhietti et al., 2011; Weddle and Retelle, 2000). It also explains the absence of ^{210}Pb in excess in the three FJS2017 cores. Hence, ^{210}Pb could not be used to derive sedimentation rates in those old sediments.

A similar stratigraphic sequence about the Champlain Sea Clay is observed through borehole descriptions of the studies quoted above:

- 1) Till that lies on the bedrock;
- 2) Locally slightly interbedded, blue-grey, silty clay sometimes with marine shells and some lumps of organic matter, odour of sulfur dioxide;
- 3) Blue-grey massive silty clay with occasional layers of sand;
- 4) Brown-olive clays interbedded with thin silty layers;
- 5) Recent sand, gravel, pebbles, alluvium and delta sediments.

By comparing the present study to the sequences listed above, the unlaminated short sedimentary cores (i.e. subunit 3a) correspond to the stratigraphic sequences 2 and 3, while the laminated cores (i.e. subunit 3b) correspond to the sequence 4. This difference between the two core types is moreover observed by the carbon analysis (Fig. 17) and water contents (Fig. 19) of the short sedimentary cores # 19-16-07-03. The laminated cores indeed present more internal variations of those two parameters. The laminations also affect the velocity and the wet bulk density of the subsurface samples. This difference is probably related to the silty nature of the laminations, compared to the more homogeneous composition of the unlaminated cores.

The previous work of Duhaime et al. (2013) demonstrates that the clays on the Montreal Island are composed of ~6% of carbonates, while the surface samples of the present study are composed of 0.1 to 1.6 % of inorganic carbon (corresponding to 0.8 to 12.3 % in carbonate equivalent). The variation in carbonates is normal in this heterogeneous environment and thus coherent with previous studies of the clays in this sector. The values of the total carbon content (0.5 to 2.3 %) of the surface samples and the

cores # 19-16-03 are also normal for marine clay. They are comparable to the values measured in the Laflamme Sea clays by St-Onge and Hillaire-Marcel (2001).

The massive aspect of subunit 3a suggests that its deposition occurred during an episode of rapid retreat of the LIS. Nutz et al. (2014) and Normandeau et al. (2013) proposed the same mechanism of deposition for a similar seismic unit. Then, subunit 3b was probably deposited during a deceleration in rates of ice-retreat or stabilization of a more distant ice-margin. A lower energy environment and a higher supply of terrestrial inputs would explain the laminated nature of subunit 3b (Cronin et al., 2008). The tabular and very high amplitude reflections downstream core # 30 (Fig. 22 – upper panel) could be the result of episodic meltwater plumes that brought coarser sediments and created a denser layer or local erosion filled by coarse sediments as paleo-channels parallel to the survey.

All those results indicate that the clays sampled on the floor of the waterway of the St. Lawrence River were deposited during the marine episode of the Champlain Sea. Local veneers of coarse and recent sediments are sometimes present over the clays (also described by Carrier et al. (2013)), but no sedimentation of fine grains occurs nowadays. In fact, the waterway is mostly in erosion due to the strong bottom currents.

1.6.2 The erosion trend of the waterway

The migrating dunes, ribbons, furrows and other ripples downstream Ste-Thérèse Island usually have shape corresponding to the general bedform distribution model or the low-sand supply model (Figs 8d and 23). Moreover, the mean migration rate of the large dunes (1.54 m/yr) is notably smaller compared to other studies with similar dune shapes and rate flow (ex: W. Finkl and Makowski, 2016 or Traini et al., 2012). This fact supports the interpretation of a low sedimentation model in the waterway, as indicated by the mean sedimentation presented in the results and the numerous profiles that testify to the local effect of erosion. On the other hand, the bathymetric analyses indicate an erosional trend observed in most part of the waterway (downstream Ste-Thérèse Island). The long-term

visible dredging marks (Fig. 8) also indicate the absence of sedimentation over them. The dredging marks and the fields of linear dunes are always located near the sides of the waterway. Sometimes, the dredging marks seem to disappear and progressively change into small linearly-aligned dunes (Fig. 8g). These are interpreted as ancient dredging marks on which little accumulation of recent sediments occurs. It explains the atypical morphology of those dunes and their stable state. The erosional trend observed in the present study is supported by the study of Rondeau et al. (2000) which suggested that 70% of the sediment load measured at the end of the studied area (Les Grèves) comes from internal sources of the St. Lawrence itself. They explain that the two main causes of erosion are the waves generated by the ships and the wind (eroding the banks of the river), and the high current velocity inside the navigation channel that is 2-3 times greater than outside the channel. However, Gaskin et al. (2003) specify that the waves are the dominant erosion mechanism because the undisturbed and unweathered Champlain Sea Clay are very resistant to bed erosion (critical shear stress of 350-450 Pa). Hence, the majority of the sediments in suspension possibly deposit in shallow zones as indicate Carignan and Lorrain (2000) (close to the shore) or even in deeper basins like the Lake Saint-Pierre or in the St. Lawrence Estuary which present major depressions filled with quaternary deposits (Duchesne et al., 2007; St-Onge et al., 2011; St-Onge et al., 2008).

1.6.3 Geomorphological features and the sediment composition of the river floor

According to Middleton and Southard (1984), and Reineck and Singh (2012), the velocity of the current in the waterway (1 m/s and faster) combined to the sediment granulometry would create large ripples, upper plane laminations, dunes, sand-waves or antidunes. The shear stress on the river bed also influences the sediment transport and the dune migrations. However, the water depth (10 m or deeper) prevents the formation of antidune. Indeed, the hydraulic regime could not reach a supercritical Froude number ($Fr > 1$), which is essential to antidune formation (Núñez-González and Martín-Vide, 2011),

because the actual bathymetry is always too deep. This relationship is governed by the following Equation 1:

Equation 1: Froude number (Park and al. 2019)

$$Fr = \frac{U_m}{\sqrt{g \times h}} = \frac{1 \text{ m/s}}{\sqrt{9.81 \text{ m/s}^2 \times 10 \text{ m}}} = 0.1$$

U_m : mean velocity of the current (m/s)

g : gravity (9.81 m/s^2)

h : height of the water column (m)

The Reynolds number however indicates that the current is turbulent ($Re > 2000$) according to the Equation 2:

Equation 2: Reynolds number (Park and al. 2019)

$$Re = \frac{U_m \times h}{v} = \frac{1 \text{ m/s} \times 10 \text{ m}}{10^{-6} \text{ m}^2/\text{s}} = 10^6$$

U_m : mean velocity of the current (m/s)

h : height of the water column (m)

v : cinematic viscosity of water ($\approx 10^{-6} \text{ m}^2/\text{s}$)

Those two parameters classify the current as subcritical-turbulent. The Froude number is a ratio between inertial and gravitational forces. A value < 1 (subcritical threshold) means that the water in movement does not have enough kinetic energy to outdo the gravity when it encounters an obstacle on the riverbed and consequently could not create braking wave. The Reynolds number is a ratio between inertial and viscous forces. A value > 2000 (turbulent threshold) means that the water particles moves in a non linear pattern along the current because the viscosity of the water is weak compared to the velocity of the current. The visible bedforms along the waterway (Fig. 24) correspond to the literature for subcritical-turbulent flow (e.g., Reading, 2009; Reineck and Singh, 2012; Traini et al., 2012). The Fig. 12 also demonstrates the influence of complex water

movements related to these particular hydrodynamic conditions. The scattered fields of medium dunes located between Jacques-Cartier wharf and the end of Boucherville's Islands (zones 1 to 5) appear to be gravel waves (Fig. 23a). Those gravel waves indicate the presence of very coarse sediments in the upper part of the waterway. This interpretation is supported by the morphology of the dunes (Fig. 12) observed with the bathymetric data and by the subbottom profiles (Figs 21 and 22) which indicate the outcrop of rock or very coarse sediments. The *ArcGIS* borehole B_2552 is located at less than 5 m of the profile #10, which passes through a medium dunes field in the zone of interest #5. It proves that the subsurface is composed of coarse sediments (till and sand layers), while the bedrock (shale) is 6 m under the riverbed. Furthermore, coring had been attempted on this section of the waterway during the FJS2017 mission, but the corer tip broke two times due to the hardness of the riverbed. The bedform morphology could in consequence be used as an indicator of the subsurface sediment nature. For example, ribbons and furrows are usually associated with coarse sediments (sand and gravel) and/or strong currents, and otherwise indicate a possible lack of sediments supply (Traini et al., 2012).

Figure 12 illustrates a sandbank typical of high-sand supply model as illustrated in figure 23c. This high-sediment supply model corresponds to the morphologies found in the zones of interest # 1-4-5. The regional analysis of the bathymetry also indicates that annual accumulations can reach 14 cm/yr or higher in the upper part of the waterway. The dredging works have not been taken into account because they are unlisted, not precisely described or locally restricted to shallow zones for navigation (usually 1 to 5 m²). Another indicator of the high-sediment supply for those zones is the migration rate of the gravel dunes (3.5 m/yr), which is two times higher than the migration rate of the large dunes downstream (1.54 m/yr). It is known that migration rates are correlated to the effect of strong bottom currents (Traini et al., 2012). Furthermore, the migration rates of the surimposed dunes are certainly too fast to be monitored by the methods used in this study. Measuring the migration rates of those smaller dunes could be an interesting tool to estimate the St. Lawrence River discharge.

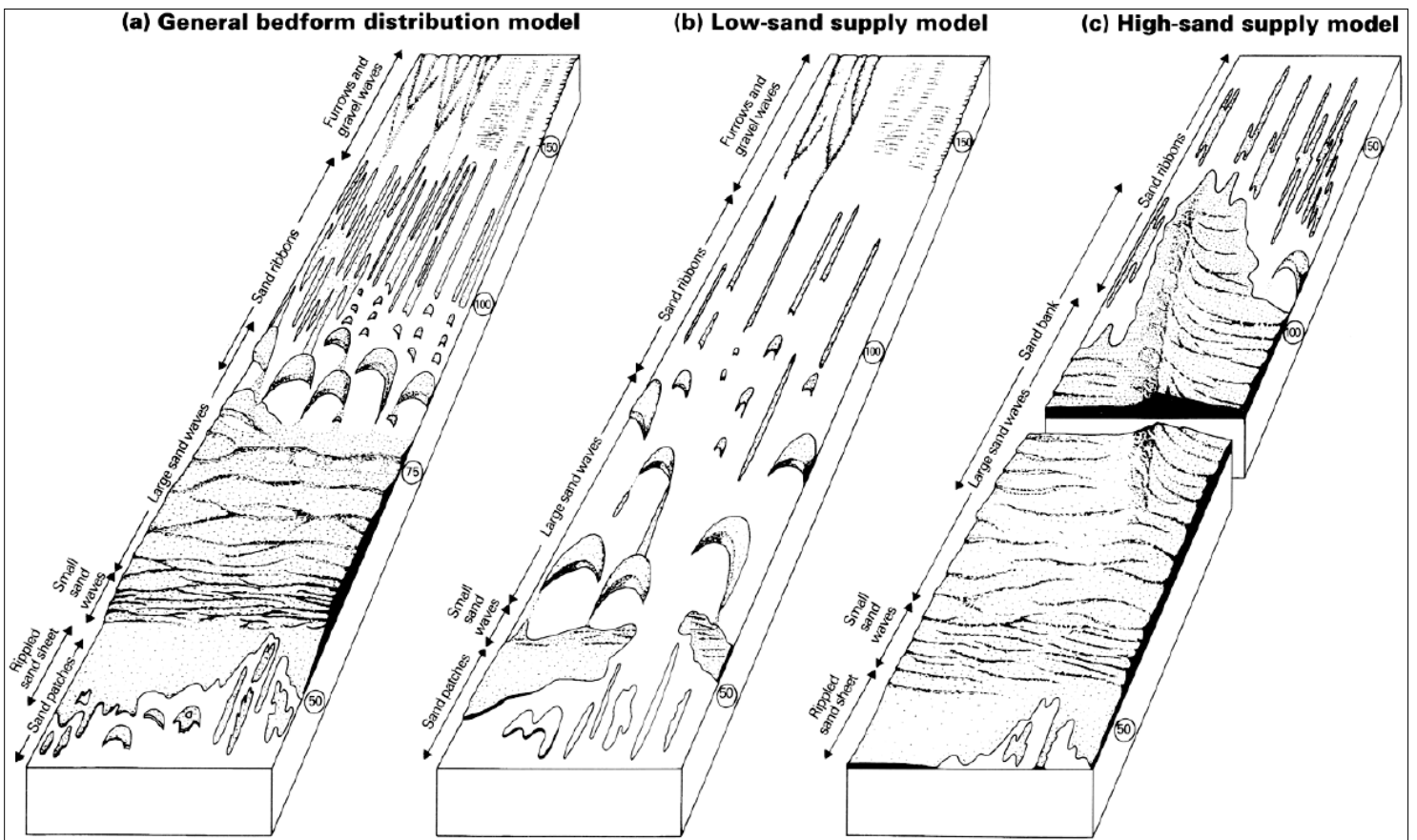


Figure 23. Distribution of the bedforms related to the current velocities (shown in cm/s within the circles) and according to Reading (2009): a) general model, b) low sand supply, and c) high sand supply model. Many bedforms of those models are visible in the waterway of the Port of Montreal.

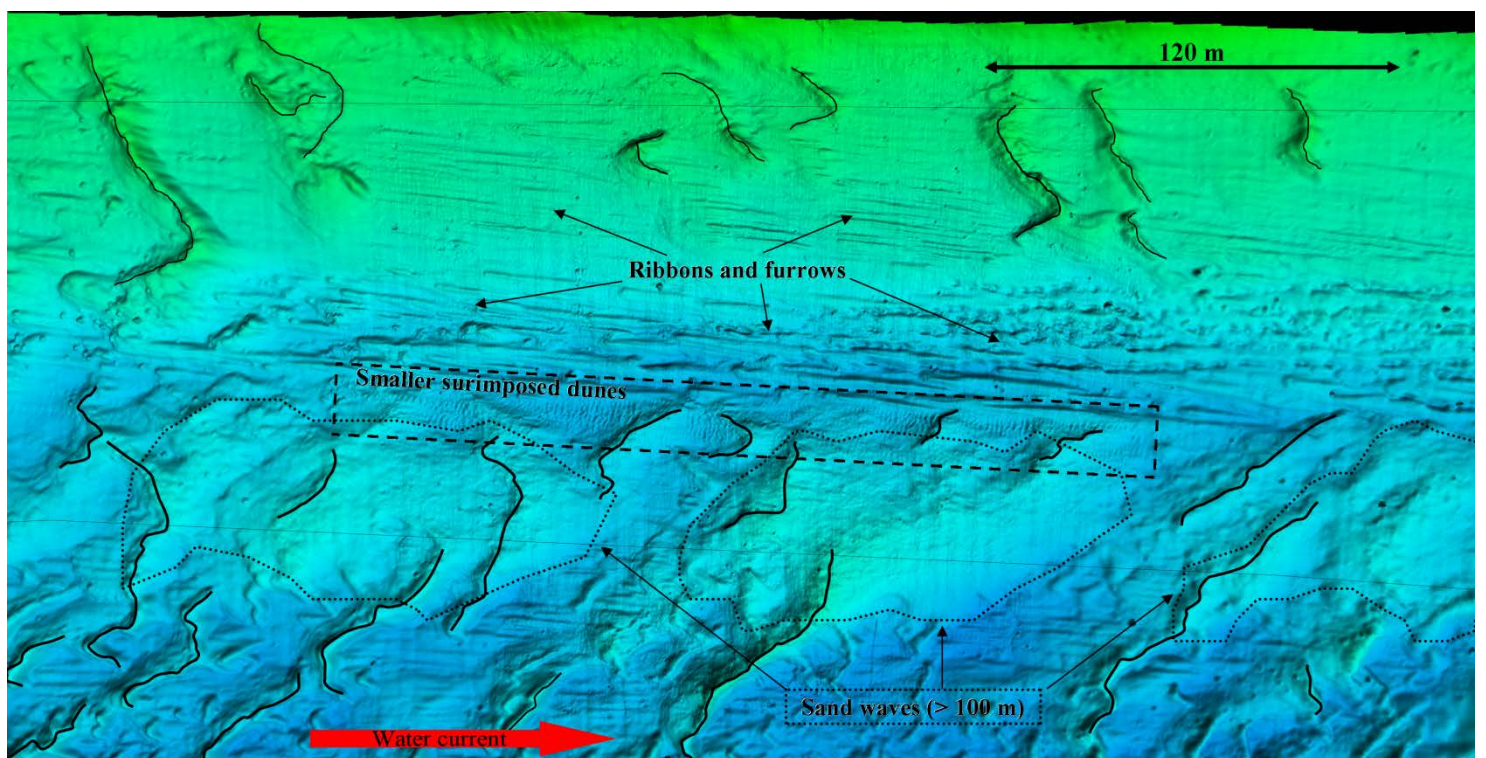


Figure 24. Bathymetry of the waterway in the zone of interest #18. See figures 3 and 4 for general location. The black full lines follow the crest of the dunes. The large dunes are usually crescent-shaped. Furrows and ribbons, sand waves and surimposed small dunes cover the riverbed. Picture obtained with the software *Caris Hips & Sips* (vertical exaggeration of 10:1).

1.7 CONCLUSIONS

The analysis of the annual multibeam data allowed the identification of geomorphological features representative of a low-supply sediment model in the waterway. The calculations made with the bathymetric profiles also provided the information that the majority of the waterway is in erosion. The nature and constancy of the subaqueous forms and the steady state of the dredging marks testify this trend. However, a question arises as to whether the low migration of dunes occurs quickly and punctually, or slowly throughout the year. The majority of the sedimentary load transported in the water column is probably deposited further Sorel-Tracy due to the strong bottom current (around 1 m/s) in the waterway or on the banks on the river. On the other hand, recurrent accumulations are found in the upper part of the waterway (i.e. the zones of interest # 1 to 5 that are located from the Jacques-Cartier wharf to the end of Boucherville's Islands). It is the principal area to be closely monitored. The other areas with possible accumulation are isolated and located close to the sides of the waterway.

The two main changes in the stratigraphy along the waterway are related to the topography of the bedrock. The Shale of Utica, which outcrops in the upper part of the study, first plunges in front of the St-Thérèse Island, where the normal "Bas-de-Sainte-Rose Fault" affects the basement rock. A change in the sedimentary processes is also observed at this point. It switches from accumulation to a global erosion trend. This change is probably related to the hydrodynamic of the river, but current profiles should be done to better understand the processes acting in this portion of the river. From there also appears the sequence of Quaternary deposits that overlies the bedrock. The short sedimentary cores obtained during the FJS2017 expedition show that the Champlain Sea Clays (unlaminated cores) outcrop until the threshold in front of the Île-aux-Prunes. This threshold is related to an uplift of the bedrock followed by another plunge of the sedimentary units. The Bouguer anomaly listed there and the presence of normal faults explain this particular topography. From that point, the short sedimentary cores become clearly laminated, but still demonstrate the outcrop of the Champlain Sea Clays. The two types of cores represent

different conditions of deposition that occurred during the last marine invasion in the St. Lawrence Lowlands.

The surface carbon contents depict values between 0.5 % and 2.3 % (TC) all along the waterway, while the mean water content is 36.0 ± 5.9 %. The short sedimentary cores are characterized by similar results (0.54 to 1.59 % TC), with little internal variations of the values for the laminated cores. This laminated trend is also visible in the water content values and it is related to the silty nature of the laminations, which is typical of the Champlain Sea Clays. The grain size distribution, the absence of ^{210}Pb in excess and the ^{14}C radiocarbon age (11 640 yr cal BP) are indicative of the Champlain Sea glaciomarine sediments. Finally, the combination of seismic data, ^{14}C age, multibeam bathymetry, borehole descriptions and the analysis of new short sedimentary cores was effective to reach the objectives of this study, yielding a modern characterization of the stratigraphy, the sediments and the sedimentary processes that are acting in the waterway between Montreal and Sorel-Tracy.

1.8 ACKNOWLEDGMENTS

This project was supported by the Port of Montreal, with special thanks to L. Dumontier, as well as NSERC through a Discovery Grant to G. St-Onge. We also thank the Canadian Hydrographic Service for the bathymetric data, the Ministry of Energy and Natural Resources of Québec (MERN) for the agreement on the *ArcGIS* framework, the Centre Interdisciplinaire de Développement en Cartographie des Océans (CIDCO) for the use of their research vessel and instruments, the marina of Verchères and their municipal administration for their permission to use the infrastructures during the FJS2017 expedition, as well as P. Lajeunesse (Laval University) and his team (especially A.-P. Trottier) for the use of their subbottom profiler and their help with data acquisition and interpretation. We also thank A. Morissette, S. Senneville, J. Caveen, L. Cavarroc, U. Neumeier and C. Rouleau (UQAR) for their help and advices at various stages of the project.

CONCLUSION GÉNÉRALE

Constats de l'étude et recommandations adressées à l'Administration du Port de Montréal

Ce travail constitue la première étude moderne axée sur le chenal de navigation du Saint-Laurent entre Montréal et Sorel-Tracy synthétisant les processus sédimentaires et la stratigraphie de cette région. Les résultats dénotent une tendance générale à l'érosion pour la zone d'étude. Les données de bathymétrie multifaisceaux ont permis l'identification de formes géomorphologiques sous-marines typiques d'un apport limité en sédiments, ou subissant de forts courants, comme le présentent les figures 8, 23 et 24. En effet, les formes de rubans et sillons, les marques de dragage, la migration lente des grandes dunes et leur géomorphologie sont des caractéristiques récurrentes au travers des données pluriannuelles de bathymétrie. Ceci confirme la tendance générale à l'érosion. Cependant, la portion amont de la zone d'étude présente des accumulations importantes par endroit. La zone d'intérêt n°1 est d'ailleurs particulièrement propice à l'accumulation, car elle occasionne jusqu'à 14 cm d'accumulation par année entre l'Île Ste-Hélène et Montréal. Toute la portion du chenal entre le quai Jacques Cartier et la fin des Îles Boucherville (zones d'intérêts n°1 à 5) est à surveiller pour maintenir la profondeur d'eau désirée. Les autres secteurs où peuvent survenir des accumulations sont isolés et accolés à la bordure du chenal.

Voici les recommandations adressées au Port de Montréal concernant la bathymétrie et les processus sédimentaires :

- Géoréférencer les travaux de dragage, car il serait ainsi possible de tenir compte de leur effet sur les futures études de la sédimentation.
- Améliorer la carte des différents types de formes sous-marines et des sédiments qui leur sont associés le long du chenal en utilisant les données de rétrodiffusion.

- Définir un protocole adapté au Port de Montréal pour optimiser l'efficacité des efforts mis dans les travaux de levés bathymétriques et leur analyse. C'est-à-dire que les analyses d'accumulation, d'érosion, les profils bathymétriques et les autres calculs effectués dans le présent travail pourraient être faits systématiquement chaque année. Établir un protocole reproductible permettrait un suivi à long terme de l'évolution des processus sédimentaires malgré une possible rotation des employés. Les améliorations ci-présentes devraient être intégrées au protocole en question.
- Un volume de sédiments déplacés pourrait être calculé à partir du suivi des crêtes des grandes dunes. Pour une plus grande précision, il faudrait par ailleurs fixer des instruments au lit de la rivière (sonar à balayage latéral ou échosondeur à haute fréquence, comme l'applique Gaudet (1990) pour l'industrie de la pêche ou utiliser un courantomètre) afin d'effectuer des mesures journalières en continu pour quantifier la migration des petites dunes surimposées qui bougent trop rapidement pour les levés saisonniers. Une autre méthode consisterait à estimer la vitesse de migration des dunes en utilisant le modèle de Bartholdy et al. (2010), qui nécessite cependant plusieurs mesures de distribution granulométrique et les caractéristiques géomorphologiques d'un champ de dunes. Il serait ensuite possible de corrélérer les déplacements des dunes de différentes grandeurs au débit de la rivière. Le travail de Traini et al. (2012) est un bon exemple des informations qui peuvent résulter de ce genre de corrélations.
- Le fait que le chenal de navigation soit majoritairement en érosion indique que les échantillons de sédiments visant à caractériser les contaminants et l'état de la pollution dans le Saint-Laurent ne doivent pas être pris dans le chenal. Les polluants se déposent principalement avec les sédiments fins et se retrouvent donc proches des berges ou dans les dépressions majeures de la voie navigable, comme le lac St-Pierre ou les fosses de l'estuaire maritime.

Ensuite, les lignes de sismique réflexion combinées aux forages décrits dans la base de données *ArcGIS* ont permis de mettre en évidence deux changements majeurs de la stratigraphie. Premièrement, le secteur amont de la zone d'étude sujet à l'accumulation correspond à l'affleurement du Shale d'Utica, parfois recouvert d'une mince couche de till. Les zones d'accumulations sont probablement les conséquences d'un régime

hydrodynamique complexe influencé par plusieurs facteurs : un débit plus grand dans le chenal sur-creusé que dans le reste de la rivière, la différence de profondeur entre le chenal et les bords de la rivière, l'étendue du lit de la rivière, les constructions humaines (canal de Beauharnois, canal de Saint-Lambert et Côte Ste-Catherine, estacade et piliers de ponts) créant de la turbulence, les rapides de Lachine, ainsi que par la rugosité du lit de la rivière reliée à la nature des sédiments. Par la suite, le Shale plonge en face de l'Île Ste-Hélène, permettant l'enregistrement des séquences quaternaires au-dessus. Cette plongée est reliée à la faille normale Bas-de-Sainte-Rose localisée dans le secteur en question. C'est également à partir de ce changement stratigraphique que la tendance globale d'érosion du chenal commence. Les échantillons obtenus durant la mission FJS2017 permettent d'affirmer que les argiles de la mer de Champlain constituent le fond du fleuve, depuis cette plongée du Shale jusqu'à l'Île-aux-Prunes (carotte n°15). Des sédiments grossiers et récents se retrouvent aussi à la surface du chenal en une mince couche discontinue. Ils forment les dunes et les autres formes naturelles visibles avec la bathymétrie. Deuxièmement, le Shale forme un seuil qui affleure à l'interface eau/sédiment en face de l'Île-aux-Prunes. Ceci constitue le deuxième changement lithologique majeur. Les argiles de la mer de Champlain constituent toujours le fond du fleuve, mais l'aspect laminé indique des conditions de sédimentation différentes entre les deux unités argileuses déposées durant la dernière invasion marine. La remontée du socle rocheux est également liée à la présence de failles normales dans ce secteur. De plus, une anomalie gravimétrique de Bouguer positive corrobore la présence du seuil.

Voici les recommandations adressées au Port de Montréal concernant les levés de sismique et de carottage pour améliorer les connaissances stratigraphiques :

- La nature du socle rocheux ou du till et des autres formations géologiques sous-jacentes sont difficiles à voir avec l'instrument de sismique choisi. Il serait conseillé de retourner faire des levés avec un instrument plus puissant et de plus faible fréquence afin de mieux différencier les structures dominantes et les unités très denses (till(s) versus socle rocheux). Ceci permettrait aussi de caractériser les secteurs où la pénétration était nulle en raison de minces couches de sédiments grossiers

modernes en surface et où l'épaisseur trop importante de sédiments glaciomarins empêchait de détecter le socle rocheux.

- Des levés à plus basse fréquence permettraient également de voir les structures internes des dunes et autres séquences sédimentaires de sous-surface. Ceci pourrait servir à interpréter les conditions de formations des formes sous-marines et l'influence des variations du débit du Saint-Laurent.
- Le tracé des levés sismiques devrait aussi être modifié. Il serait conseillé de faire des lignes parallèles au chenal. Au minimum, deux lignes devraient être faites : à l'aller, proche d'une bordure et au retour proche de l'autre bordure du chenal. La couverture permettrait ainsi de mieux visualiser le comportement des unités perpendiculairement au chenal. Ces informations pourraient servir à choisir de quel côté du chenal un approfondissement serait moins couteux, selon la topographie du roc.
- Des forages ou carottages ponctuels sur plateforme fixe seraient fortement suggérés afin de bonifier l'interprétation des données aux endroits où l'information géologique est manquante.
- La base de données de données *ArcGIS* comporte encore des erreurs, car le logiciel de reconnaissance de texte utilisé pour numériser des descriptions de milliers de forages n'était pas sans faille. Les données pourraient être soumises à des formules de détection des erreurs et d'autres outils informatiques visant l'uniformisation des systèmes de références verticales et horizontales des forages.

Les analyses des échantillons de surface montrent des teneurs en carbone (carbone total de 0.5 % à 2.3 %) et en eau (moyenne de $36.0 \pm 5.9\%$) relativement constantes tout au long de la zone d'étude. Les valeurs de ces deux paramètres également mesurés le long des trois petites carottes sédimentaires (carottes # 19-16-03) présentent aussi des valeurs normales pour les argiles marines de la mer de Champlain. Les carottes laminées, comparativement aux non laminées, montrent cependant de légères variations internes de ces valeurs. De plus, la distribution granulométrique de la majorité des échantillons est caractérisée par une dominance des argiles et des silts, avec des compositions variées en sable, gravier et cailloux. Certaines carottes présentant de grandes proportions de sédiments

grossiers ont été échantillonnées dans des champs de dunes où les différences annuelles de bathymétrie démontrent de l'érosion. Les rares carottes sédimentaires de granulométrie grossière sont plus courtes que les autres, car il était difficile et souvent impossible de faire pénétrer le carottier dans ces sédiments. Les datations effectuées sur les argiles par l'analyse du radiocarbone et de l'excès de ^{210}Pb confirment que les argiles recouvrant le fond du chenal proviennent de la mer de Champlain (11 640 cal BP).

Voici une liste de recommandations pour les campagnes d'échantillonnage futures :

- Il serait judicieux d'utiliser un carottier plus adapté aux forts courants et à la nature grossière et dense des sédiments du fond du chenal. Le *Coriolis II* serait par exemple équipé d'un carottier à piston probablement plus performant pour obtenir de longues carottes sédimentaires.
- Le diamètre des carottes sédimentaires devrait aussi être plus gros que celui utilisé (2 pouces), car les analyses ont été limitées par la quantité de sédiments disponibles. En effet, des mesures de teneurs en azote des sédiments ont été tentées, mais la très faible concentration de cet élément n'a pas pu fournir des résultats significatifs. Il aurait fallu utiliser une plus grande quantité de sédiments que ce que l'on possédait. Obtenir les valeurs de carbone, d'azote et leurs isotopes respectifs ($\delta^{13}\text{C}$ et $\delta^{15}\text{N}$) servirait à retracer l'origine de la matière organique et ainsi mieux comprendre les conditions de déposition des sédiments et leur nature (St-Onge and Hillaire-Marcel, 2001).
- De plus grosses carottes sédimentaires permettraient aussi d'augmenter la résolution de l'échantillonnage et des analyses granulométriques. Il serait recommandé d'échantillonner à tous les 0,5 cm (ou plus rapproché) les carottes laminées afin de mieux caractériser les laminations en question.

Finalement, les conclusions du présent travail apportent une caractérisation moderne du chenal de navigation entre Montréal et Sorel-Tracy. La stratigraphie, la nature des sédiments et les processus sédimentaires affectant cette voie navigable de grande importance sont décrits par la combinaison de plusieurs sources d'informations et de levés scientifiques complémentaires. Les objectifs de cette étude scientifique ont été atteints, et

entraînent, comme souvent, de nouveaux questionnements, rencontrent des limitations et mettent en évidence des améliorations possibles suggérant la poursuite des recherches nécessaires à la compréhension des changements survenant dans le fleuve Saint-Laurent. Une amélioration nécessitant peu de changements aux travaux actuels consisterait à comparer les données de rétrodiffusion aux formes du lit de la rivière. L'intérêt principal serait d'établir des corrélations entre la rétrodiffusion, les formes sous-marines et la nature des sédiments comme le présentent W.Finkl et Makowski (2016). De prochaines études pourraient aussi porter sur le lien entre le magnétisme des sédiments et leur contamination. Le travail de Pozza et al. (2004) montre qu'il est possible de détecter la contamination des sédiments sans prélèvement destructeur en utilisant un magnétomètre tracté par bateau. Ensuite, il serait important d'étudier les courants dans le chenal de navigation afin de comprendre l'influence de la morphologie du fleuve, du débit et du dragage sur la sédimentation. Il serait par exemple pertinent de modéliser l'effet d'un chenal plus profond et de prédire les effets conséquents sur l'érosion des berges ou sur la vitesse des courants de surface affectant les embarcations.

RÉFÉRENCES BIBLIOGRAPHIQUES

- Ashley, G. M. 1990. Classification of large-scale subaqueous bedforms; a new look at an old problem. *Journal of Sedimentary Research*, vol. 60(1), p. 160-172.
- Baillargeon, M.-A. 2015. Étude d'avant-projet sur la méthodologie de dragage visant à augmenter l'accessibilité aux installations portuaires. *Travaux publics et services gouvernementaux Canada, Québec*, Projet n° R.067499.001 (Préliminaire)
- Bard, E., Arnold, M., Mangerud, J., Paterne, M., Labeyrie, L., Duprat, J., Mélières, M.-A., Sønstegaard, E., and Duplessy, J.-C. 1994. The North Atlantic atmosphere-sea surface ^{14}C gradient during the Younger Dryas climatic event. *Earth and Planetary Science Letters*, vol. 126(4), p. 275-287. doi:10.1016/0012-821X(94)90112-0
- Bartholdy, J., Ernstsen, V. B., Flemming, B. W., Winter, C., and Bartholomä, A. 2010. A simple model of bedform migration. *Earth Surface Processes and Landforms*, vol. 35(10), p. 1211-1220.
- Blott, S. J. and Pye, K. 2001. GRADISTAT: a grain size distribution and statistics package for the analysis of unconsolidated sediments. *Earth Surface Processes and Landforms*, vol. 26(11), p. 1237-1248. doi:10.1002/esp.261
- Bouchard, A. and Cantin, J.-F. (2015). Changes in water levels and flows in the St. Lawrence River. *Meteorological Service of Canada*. [Retrieved from] http://planstlaurent.qc.ca/en/state_monitoring/monitoring_sheets/changes_in_water_levels_and_flows_in_the_st_lawrence_river.html
- Bourque, P.-A. 2004. Le Quaternaire au Québec: une histoire de glaciations-déglaciations. *Département de Géologie et de génie géologique - Planète Terre*. Université Laval. [Retrieved from] <http://www2.ggl.ulaval.ca/personnel/bourque/s5/5.5.quaternaire.html>
- Brouard, E., Lajeunesse, P., Cousineau, P. A., Govare, É., and Locat, J. 2016. Late Wisconsinan deglaciation and proglacial lakes development in the Charlevoix region, southeastern Québec, Canada. *Boreas*, vol. 45(4), p. 754-772. doi:10.1111/bor.12187
- Carignan, R. and Lorrain, S. 2000. Sediment dynamics in the fluvial lakes of the St. Lawrence River: accumulation rates and characterization of the mixed sediment layer. *Canadian Journal of Fisheries and Aquatic Sciences*, vol. 57(S1), p. 63-77. doi:10.1139/f99-246
- Carrier, M.-A., Lefebvre, R., Rivard, C., Parent, M., Ballard, J. M., Vigneault, H., and Gloaguen, E. 2013. Portrait des ressources en eau souterraine en Montérégie Est,

- Québec, Canada. *Ministère du Développement durable, de la Faune et des Parcs du Québec. INRS-ETE, CGC, OBV Yamaska, IRDA, Québec*, 319 p.
- Catana, M. C. 2006. Compaction and water retention characteristics of Champlain sea clay. (Thesis), *University of Ottawa, Departement of Civil Engineering*. 24 p.
- Cauchon-Voyer, G., Locat, J., and St-Onge, G. 2008. Late-Quaternary morpho-sedimentology and submarine mass movements of the Betsiamites area, Lower St. Lawrence Estuary, Quebec, Canada. *Marine Geology*, vol. 251(3–4), p. 233-252. doi:<http://dx.doi.org/10.1016/j.margeo.2008.03.003>
- Chen, Z., Lavoie, D., and Malo, M. 2014. Caractéristiques géologiques et évaluation des ressources pétrolières du Shale d'Utica, Québec, Canada. (Dossier Public 7625). *Canada Geological Survey*. doi. 10.4095/293930.
- Cronin, T. M., Manley, P. L., Brachfeld, S., Manley, T. O., Willard, D. A., Guilbault, J. P., Rayburn, J. A., Thunell, R., and Berke, M. 2008. Impacts of post-glacial lake drainage events and revised chronology of the Champlain Sea episode 13–9 ka. *Palaeogeography, Palaeoclimatology, Palaeoecology*, vol. 262(1), p. 46-60. doi:<https://doi.org/10.1016/j.palaeo.2008.02.001>
- Cutshall, N. H., Larsen, I. L., and Olsen, C. R. 1983. Direct analysis of ^{210}Pb in sediment samples: Self-absorption corrections. *Nuclear Instruments and Methods in Physics Research*, vol. 206(1), p. 309-312. doi:[https://doi.org/10.1016/0167-5087\(83\)91273-5](https://doi.org/10.1016/0167-5087(83)91273-5)
- Dion, D. 1977. Levé géotechnique de la région de Boucherville-Tracy. Rapport d'étude et cartes d'aptitude. *Ministère des Richesses Naturelles du Québec. Direction générale des mines. DPV-499*, vol. 1
- Dolgopolova, E. N. and Isupova, M. V. 2011. Water and sediment dynamics at Saint Lawrence River mouth. *Water Resources*, vol. 38(4), p. 453-469. doi:[10.1134/s009780781104004x](https://doi.org/10.1134/s009780781104004x)
- Dubé-Loubert, H., Parent, M., and Brazeau, A. 2014. Cartographie des dépôts de surface des bassins versant contigus des rivières Richelieu, Yamaska et de la baie Missisquoi. (RG 2014-01). *Ministère du Développement durable, de l'Environnement, de la Faune et des Parcs. Bibliothèque et Archives nationales du Québec*. 26 p.
- Duchesne, M., Pinet, N., Bolduc, A., Bédard, K., and Lavoie, D. 2007. Seismic stratigraphy of the lower St Lawrence River estuary (Quebec) Quaternary deposits and seismic signature of the underlying geological domains. *Current Research. Geological Survey of Canada*. 16 p.
- Duhaime, F., Benabdallah, E. M., and Chapuis, R. P. 2013. The Lachenaie clay deposit: some geochemical and geotechnical properties in relation to the salt-leaching process. *Canadian Geotechnical Journal*, vol. 50(3), p. 311-325. doi:[10.1139/cgj-2012-0079](https://doi.org/10.1139/cgj-2012-0079)

- Ferland, P. and Occhietti, S. 1990. L'Argile de la Pérade: nouvelle unité marine antérieure au Wisconsinien supérieur, vallée du Saint-Laurent, Québec. *Géographie physique et Quaternaire*, vol. 44(2), p. 159-172.
- Fortin, D., Francus, P., Gebhardt, A. C., Hahn, A., Kliem, P., Lisé-Pronovost, A., Roychowdhury, R., Labrie, J., and St-Onge, G. 2013. Destructive and non-destructive density determination: method comparison and evaluation from the Laguna Potrok Aike sedimentary record. *Quaternary Science Reviews*, vol. 71, p. 147-153. doi:<https://doi.org/10.1016/j.quascirev.2012.08.024>
- François, Catherine. 2015. *La technologie au service des pilotes du Saint-Laurent. Radio-Canada*. [Retrieved from] <http://ici.radio-canada.ca/nouvelle/729874/formation-pilotes-fleuve-saint-laurent-simulation>
- Gadd, N. R. 1971. Pleistocene Geology of the Central St. Lawrence Lowland - with Selected Passages from an Unpublished Manuscript: The St. Lawrence Lowland, by J.W. Goldthwait. *Geological Survey of Canada. Department of Energy, Mines and Resources*. Memoir 359. Ottawa, Canada. 165 p.
- Gaudet, D. M. 1990. Enumeration of migrating salmon populations using fixed-location sonar counters. *Rapports et Proces-Verbaux des Reunions, Conseil International pour l'Exploration de la Mer*, vol. 187, p. 197-209
- Gaskin, S. J., Pieterse, J., Al Shafie, A., and Lepage, S. 2003. Erosion of undisturbed clay samples from the banks of the St. Lawrence River. *Canadian Journal of Civil Engineering*, vol. 30(3), p. 585. doi:10.1139/l03-008
- Gélard, J.-P., Jébrak, M., and Prichonnet, G. 1992. Les contraintes phanérozoïques dans la plate-forme du Saint-Laurent, région de Montréal, Québec. *Canadian Journal of Earth Sciences*, vol. 29(3), p. 499-505
- Globensky, Y. 1987. *Géologie des Basses-Terres du Saint-Laurent*. Ministère de l'énergie et des ressources du Québec, Québec, 63 p.
- Godin, G. 1999. The Propagation of Tides up Rivers With Special Considerations on the Upper Saint Lawrence River. *Estuarine, Coastal and Shelf Science*, vol. 48(3), p. 307-324. doi:10.1006/ecss.1998.0422
- Golder Associés Ltée. 2009. Reorganization of Sections 25 to 57, Port of Montreal. Factual Report, submitted to Moffat & Nichol. *Golder Associés Ltée*. Montreal, Canada. 290 p.
- Gouvernement of Canada. 2001. Field data for the mapping of wetlands in the St. Lawrence River between Cornwall and Trois-Pistoles, 2000-2001 [CSV]. *Wetlands-StLawrenceRiver-Inventory-2000-2001.csv*, Environment and natural resources Canada [Retrieved from] <https://open.canada.ca/data/en/dataset/e2c8aa2e-fe17-4bd5-92ce-1462460cc330>

- Government of Canada. 2019. Hydrometric Station and Network Data. *Environment and natural resources Canada* [Retrieved from] https://wateroffice.ec.gc.ca/mainmenu/station_and_network_data_index_e.html
- Gouvernement du Québec. 2019. SIGÉOM - Carte interactive. Ministère de l'Énergie et des ressources naturelles du Québec. [Retrieved from] http://sigeom.mines.gouv.qc.ca/signet/classes/I1102_indexAccueil
- Heiner, J. and Scott, L. 1999. Late glacial stratigraphy and history of the Gulf of St. Lawrence, Canada. *Canadian Journal of Earth Sciences*, vol. 36(8), p. 1327-1345. doi:10.1139/e99-030
- Hélie, J. F. 2004. Géochimie et flux de carbone organique et inorganique dans les milieux aquatiques de l'est du Canada: exemples du Saint-Laurent et du réservoir Robert-Bourassa - Approche isotopique. (Ph.D.), *University of Quebec at Montreal*, Library and Archives Canada. 221 p.
- Hitchcock, E. 1831. Report on the Geology of Vermont. vol. 1, 568 p.
- Intergovernmental Panel on Climate Change et al. 2014. Climate change 2014: synthesis report. Contribution of Working Groups I, II and III to the fifth assessment report of the Intergovernmental Panel on Climate Change. *IPCC*, Geneva, Switzerland, 151 p.
- Lamontagne, L., Martin, A., Grenon, L., and Cossette, J.-M. 2000. Étude pédologique du comté de Laprairie (Québec). *Centre de recherche et de développement sur les sols et les grandes cultures*, Direction générale de la recherche, Agriculture et Agroalimentaire Canada, Sainte-Foy Quebec. Bulletin d'extension n° 11. 356 pp.
- Lamothe, M. 1985. Lithostratigraphy and geochronology of the Quaternary deposits of the Pierreville and St-Pierre Les Becquets areas, Quebec. (Doctor), *University of Western Ontario*, London, Ontario. 249 p.
- Lamothe, M. and St-Jacques, G. 2015. Géologie du Quaternaire des bassins versants des rivières Nicolet et Saint-François, Québec. MB-2015-01. Département des sciences de la Terre et de l'Atmosphère, *Université du Québec à Montréal*. Présenté au *Ministère des Ressources Naturelles et de la Faune*. 38 p.
- LaSalle, P. 1963. Géologie des dépôts meubles de la région de Verchères, comtés de Joliette, Berthier, L'Assomption, Richelieu, Verchères et Saint-Hyacinthe : rapport préliminaire. Québec: *Ministère des richesses naturelles*. [Retrieved from] <https://books.google.ca/books?id=gFxjtAEACAAJ>
- LaSalle, P. and Elson, J. A. 1962. Rapport préliminaire sur la région de Beloeil - Géologie des dépôts meubles, comptés de l'Assomption, Bourget, de Verchères, de St-Hyacinthe, de Chambly et de Rouville. *Ministère des richesses naturelles, service des eaux, gaz et pétrole du Québec, Canada*. R.P. NO 497. 13 p.
- Lavoie, D. et al. 2014. The Utica Shale and gas play in southern Quebec: Geological and hydrogeological syntheses and methodological approaches to groundwater risk

- evaluation. *International Journal of Coal Geology*, vol. 126, p. 77-91. doi:10.1016/j.coal.2013.10.011
- Leclerc, M. et al. 1991. Fleuve Saint-Laurent Modélisation intégrée du suivi de la qualité de l'eau du tronçon Tracy : Lac Saint-Pierre : Rapport no 1, vol. 1 - Tome 2: Annexe infographique : Atlas numérique des courants et autre caractéristiques des écoulements en eau libre du tronçon Tracy : Lac Saint-Pierre. *INRS-Eau, Terre et Environnement, Sainte-Foy, Québec*. 138 p.
- Logan, S. W. E. 1862. *Geology of Canada*.
- Middleton, G. V. and Southard, J. B. 1984. Mechanics of Sediment Movement. *SEPM*. 401 p.
- Montreal Port Authority. (2019). Statistics. [Retrieved from] <https://www.port-montreal.com/PMStats/html/frontend/statistics.jsp?lang=en&context=community>
- Normandeau, A., Lajeunesse, P., and Philibert, G. 2013. Late-Quaternary morphostratigraphy of Lake St-Joseph (southeastern Canadian Shield): Evolution from a semi-enclosed glacimarine basin to a postglacial lake. *Sedimentary Geology*, vol. 295(2013), p. 38-52. doi:10.1016/j.sedgeo.2013.07.005
- Normandeau, A., Lajeunesse, P., and St-Onge, G. 2015. Submarine canyons and channels in the Lower St. Lawrence Estuary (Eastern Canada): Morphology, classification and recent sediment dynamics. *Geomorphology*, vol. 241, p. 1-18. doi:<https://doi.org/10.1016/j.geomorph.2015.03.023>
- Normandeau, A., Lajeunesse, P., Trottier, A.-P., Poiré, A. G., and Pienitz, R. 2017. Sedimentation in isolated glacimarine embayments during glacio-isostatically induced relative sea level fall (northern Champlain Sea basin). *Canadian Journal of Earth Sciences*, vol. 54(10), p. 1049-1062. doi:10.1139/cjes-2017-0002
- Núñez-González, F. and Martín-Vide, J. P. 2011. Analysis of antidune migration direction. *Journal of Geophysical Research: Earth Surface*, vol. 116(F2). doi:10.1029/2010JF001761
- Nutz, A. et al. 2014. Seismic-stratigraphic record of a deglaciation sequence: from the marine Laflamme Gulf to Lake Saint-Jean (late Quaternary, Québec, Canada). *Boreas*, vol. 43(2), p. 309-329. doi:10.1111/bor.12039
- Occhietti, S. 1990. Lithostratigraphie du Quaternaire de la vallée du St-Laurent : méthode, cadre conceptuel et séquences sédimentaires. *Géographie physique et Quaternaire*, vol. 44(2), p. 137-145. doi:10.7202/032813ar
- Occhietti, S., Chartier H., M., Hillaire-Marcel, C., Cournoyer, M., L. Cumbaa, S., and Harington, R. 2001. Paléoenvironnements de la mer de Champlain dans la région de Québec, entre 11 300 et 9750 bp : le site de Saint-Nicolas. *Géographie physique et Quaternaire*, vol. 55(1), p. 23-46. doi:10.7202/005660ar

- Occhietti, S., Parent, M., Lajeunesse, P., Robert, F., and Govare, É. 2011. Chapter 47 - Late Pleistocene-Early Holocene Decay of the Laurentide Ice Sheet in Québec-Labrador. In J. Ehlers, P. L. Gibbard, and P. D. Hughes (Eds.), *Elsevier: Developments in Quaternary Sciences*, vol. 15, p. 601-630.
- Occhietti, S. and Richard, P. 2003. Effet réservoir sur les âges 14C de la Mer de Champlain à la transition Pléistocène-Holocène : révision de la chronologie de la déglaciation au Québec méridional. *Géographie physique et Quaternaire*, vol. 57(2-3), p. 115-138. doi:<https://doi.org/10.7202/011308ar>
- Painchaud, J. and Villeneuve, S. 2003. Portrait global de l'état du Saint-Laurent-L'eau, les sédiments, les ressources biologiques et les usages. *Direction du suivi de l'état de l'environnement, ministère de l'Environnement, Québec, et Direction de la conservation de l'environnement, Environnement Canada, Québec*. 18 p.
- Parent, M. and Occhietti, S. 1988. Late Wisconsinan Deglaciation and Champlain Sea Invasion in the St. Lawrence Valley, Québec. *Géographie physique et Quaternaire*, vol. 42(3), p. 215. doi:[10.7202/032734ar](https://doi.org/10.7202/032734ar)
- Park, S. W., Hwang, J. H., and Ahn, J. 2019. Physical Modeling of Spatial and Temporal Development of Local Scour at the Downstream of Bed Protection for Low Froude Number. *Water*, vol. 11(5), p. 1041.
- Pelletier, M. 2005. La contamination des sédiments par les toxiques-le lac Saint-Pierre: dernière halte avant l'estuaire. (0662706749). *Gouvernement du Québec*. doi. 0-662-70674-9.
- Pozza, M. R., Boyce, J. I., and Morris, W. A. 2004. Lake-based magnetic mapping of contaminated sediment distribution, Hamilton Harbour, Lake Ontario, Canada. *Journal of Applied Geophysics*, vol. 57(1), p. 23-41. doi:[10.1016/j.jappgeo.2004.08.005](https://doi.org/10.1016/j.jappgeo.2004.08.005)
- Prest, V. K., Keyser, J. H., Prest, V. K., and Hode-Keyser, J. 1982. Caractéristiques géologiques et géotechniques des dépôts meubles de l'île de Montréal et des environs, Québec. *Commission géologique du Canada, Ministère des approvisionnements et services*, Ottawa. 29 p.
- Reading, H. G. 2009. Sedimentary environments: processes, facies and stratigraphy. John Wiley & Sons, *University of Oxford*, 669 p.
- Reineck, H. E. and Singh, I. B. 2012. Depositional Sedimentary Environments: With Reference to Terrigenous Clastics. *Springer Berlin Heidelberg*. 549 p.
- Rondeau, B., Cossa, D., Gagnon, P., and Bilodeau, L. 2000. Budget and sources of suspended sediment transported in the St. Lawrence River, Canada. *Hydrological Processes*, vol. 14(1), p. 21-36. doi:[10.1002/\(sici\)1099-1085\(200001\)14:1<21::aid-hyp907>3.0.co;2-7](https://doi.org/10.1002/(sici)1099-1085(200001)14:1<21::aid-hyp907>3.0.co;2-7)
- Rosset, P. and Chouinard, L. E. 2009. Characterization of site effects in Montreal, Canada. *Natural Hazards*, vol. 48(2), p. 295-308. doi:[10.1007/s11069-008-9263-1](https://doi.org/10.1007/s11069-008-9263-1)

- Russell, H. A. J. and Cummings, D. I. 2009. Deglaciation Of The Champlain Sea Basin, Eastern Ontario. *Geological Survey of Canada*. Field-Trip Report. 72nd - Friends of The Pleistocene Reunion, Ottawa, Ontario. 70 p.
- San Miguel, E. G., Pérez-Moreno, J. P., Bolívar, J. P., García-Tenorio, R., and Martin, J. E. 2002. ^{210}Pb determination by gamma spectrometry in voluminal samples (cylindrical geometry). *Nuclear Instruments and Methods in Physics Research Section A: Accelerators, Spectrometers, Detectors and Associated Equipment*, vol. 493(1), p. 111-120. doi:[https://doi.org/10.1016/S0168-9002\(02\)01415-8](https://doi.org/10.1016/S0168-9002(02)01415-8)
- Schock, S. G., LeBlanc, L. R., and Mayer, L. A. 1989. Chirp subbottom profiler for quantitative sediment analysis. *Geophysics*, vol. 54(4), p. 445-450.
- Séjourné, S., Dietrich, J. R., and Malo, M. 2002. New interpretations of industry seismic lines, southern Quebec Appalachians foreland. Current Research 2002-D1. *Geological Survey of Canada*. 10 p.
- Séjourné, S., Malet, X., Lefebvre, R., and Lavoie, D. 2013. Synthèse hydrogéologique du Shale d'Utica et des unités sus-jacentes (Lorraine, Queenston et dépôts meubles), Basses-Terres du Saint-Laurent, Québec. *Commission géologique du Canada*, Dossier Public 7338, 165 p. doi:10.4095/292430
- Société de développement économique du Saint-laurent. 2013. Corridor de commerce Saint-Laurent—Grands Lacs. *Voie d'accès à la prospérité économique*. [Retrieved from] http://www.st-laurent.org/wp-content/uploads/2015/03/etude_corridor_hiver2013_francais_complet_comprime_0.pdf
- St-Onge, G., Duchesne, M. J., and Lajeunesse, P. 2011. Marine geology of the St. Lawrence Estuary. *IOP Conference Series: Earth and Environmental Science*, vol. 14. doi:10.1088/1755-1315/14/1/012003
- St-Onge, G. and Hillaire-Marcel, C. 2001. Isotopic constraints of sedimentary inputs and organic carbon burial rates in the Saguenay Fjord, Quebec. *Marine Geology*, vol. 176(1), p. 1-22. doi:[https://doi.org/10.1016/S0025-3227\(01\)00150-5](https://doi.org/10.1016/S0025-3227(01)00150-5)
- St-Onge, G., Lajeunesse, P., Duchesne, M. J., and Gagné, H. 2008. Identification and dating of a key Late Pleistocene stratigraphic unit in the St. Lawrence Estuary and Gulf (Eastern Canada). *Quaternary Science Reviews*, vol. 27(25–26), p. 2390-2400. doi:<http://dx.doi.org/10.1016/j.quascirev.2008.08.02>
- St-Onge, G. and Long, B. 2009. CAT-scan analysis of sedimentary sequences: An ultrahigh-resolution paleoclimatic tool. *Engineering Geology*, vol. 103, p. 127-133. doi:10.1016/j.enggeo.2008.06.016
- St-Onge, G., Mulder, T., Francus, P., and Long, B. 2007. Chapter Two : Continuous Physical Properties of Cored Marine Sediments. In C. Hillaire-Marcel A. De Vernal (Eds.), *Elsevier: Developments in Marine Geology*, vol. 1, p. 63-98.

- Syvitski, J. P. M. and Praeg, D. B. 1989. Quaternary sedimentation in the st. Lawrence estuary and adjoining areas, eastern Canada: An overview based on high resolution seismo-stratigraphy. *Géographie physique et Quaternaire*, vol. 43(3), p. 291-310.
- Talbot, A. d. 2006. Enjeux de la disponibilité de l'eau pour le fleuve Saint-Laurent – Synthèse environnementale. *Environnement Canada*, Montréal. 215 p. [Retrieved from] http://belsp.uqtr.ca/523/1/Talbot%20et%20al_2006_disponibilite_eau_Saint-Laurent_A.pdf doi. No de catalogue En154-43/2006F
- The Royal Canadian Geographical Society. 2019. Fleuve Saint-Laurent (Plaines de forêts mixtes). *Les Rivières du Canada*, Online Atlas. [Retrieved from] http://www.canadiangeographic.com/atlas/themes.aspx?id=rivers&sub=rivers_east_stlawrence&lang=Fr
- Thériault, R. 2012. Caractérisation du Shale d'Utica et du Groupe de Lorraine, Basses-Terres du Saint-Laurent-Partie 2: Interprétation géologique. DV 2012-04. *Geologie Québec, Ressources naturelles et faunes*. 80 p.
- Tougas-Tellier, M.-A., Morin, J., Hatin, D., and Lavoie, C. 2013. Impacts des changements climatiques sur l'expansion du roseau envahisseur dans les frayères du fleuve Saint-Laurent. *Ouranos, Fonds vert Québec*, Montréal. 53 p.
- Traini, C., Schrottke, K., Stattegger, K., Dominguez, J., Kacenelenbogen Guimaraes, J., Vital, H., Beserra, D., and Aquino da Silva, A. 2012. Morphology of Subaqueous Dunes at the Mouth of the Dammed River Sao Francisco (Brazil). *Journal of Coastal Research*, vol. 28(6), p. 1580-1590. doi:10.2112/jcoastres-d-10-00195.1
- W. Finkl, C. and Makowski, C. 2016. Seafloor Mapping along Continental Shelves : Research and Techniques for Visualizing Benthic Environments. *Springer*, vol. 13. Switzerland, 297 p.
- Weddle, T. K. and Retelle, M. J. 2000. Deglacial history and relative sea-level changes, northern New England and adjacent Canada. *Geological Society of America*, vol. 351.
- Woodley, M. A. 1996. An investigation of pore water in Champlain Sea deposits at Mer Bleue Ottawa, Canada (Thesis). *Department of Earth Sciences, Carleton University* Ottawa, Ontario. 140 p.
- Woodworth, J. B. 1905. Ancient water levels of the Champlain and Hudson valleys. (No. 84). *New York State Education Department*
- Zhang, D. 2000. Fluxes of Short-lived Radioisotopes in the Marginal Marine Basins of Eastern Canada. (Ph.D Thesis), *Université du Québec à Montréal*, Montréal. 193 p.

